Spring 2022

Pd-based Photocatalysts for Heck C-C Cross-Coupling Reactions

Suha Ali Alshehri
Eastern Illinois University

Pd-based Photocatalysts for Heck C-C Cross-Coupling Reactions

Suha Ali Alshehri

Research Advisor: Dr. Hongshan He

Eastern Illinois University

Department of Chemistry and Biochemistry

TABLE OF CONTENTS

Acknowledgement

First and foremost, I want to thank my research supervisor, Dr. Hongshan He, for all of his assistance during my time at EIU. His encouragement, creative, and comprehensive advice until this work came to existent. My thanks go out to the members of my thesis committee, Dr. Radu Semeniuc, Dr. Zhiqing Yan, and Dr. Michael Beck; whose so kindly participate in this research by giving generously of their time and helpful suggestions. I'd also like to thank the Department of Chemistry and Biochemistry at Eastern Illinois University for their kind assistance. Finally, I want to express my appreciation to my family, for their support and constant love.

Abbreviations

1. C-C carbon-carbon
2. SET Single electron transfer
3. EnT Energy transfer
4. PET Photo induced electron transfer
5. MLCT Metal to ligand charge transfer
6. TON Turnover number
7. TOF Turnover frequency
8. ISC Intersystem crossing
9. BODIPY Dipyrromethene boron difluoride
10. DCM Dichloromethane
11. DMF Dimethylformamide
12. DMSO Dimethyl sulfoxide
13. $CDCl_3$ Deuterated chloroform
14. TMS Tetramethylsilane
15. S Solvent
16. rt Room temperature

Abstract

Heck C-C cross-coupling reaction has been widely employed in synthetic organic chemistry because of its high efficiency and simplicity, however the conventional Heck C-C cross-coupling reaction conditions involve the use of an expensive toxicant phosphine-ligated palladium complexes, and high temperature. To address these drawbacks, a highly efficient, homogeneous photocatalyst based on BODIPY for the Heck C-C cross-coupling reactions of aryl iodide and methyl acrylate in DMF solvent under inert conditions has been developed. The 4-Py-BDP-Pd, 3-Py-BDP-Pd and, 2-Py-BOD-Pd catalysts were synthesized and purified using column chromatography. The optical properties of products and intermediates were studied by UV/vis absorption and fluorescence spectroscopy. Catalysts were used for the C-C cross-coupling reaction between iodobenzene and methyl acrylate which successfully produced a substituted alkene with high reactivities under mild condition. Heck cross-coupling reactions of a wide range of iodobenzene with methyl acrylate have been done to evaluate the substrate scope of the photocatalyzed Heck C-C cross-couplings reactions. When electron donating groups derivatives were used, desired product yields were higher than that of the model reaction. Meanwhile, lower yields were obtained when electron withdrawing groups were used.

List of Figures

List of Tables

1 Introduction

1.1 Heck Reactions

1.1.1 Heck Reactions and its applications

The construction of C-C bond has played a crucial role in the synthesis of organic chemistry. Extensive efforts were made to develop more convenient and efficient method to the field of C-C bond formation.[1] Some examples of these coupling reactions are aldol reactions[2], Grignard reaction[3], a Wittig reaction[4] and a Michael reaction[5]. After the use of organometallic catalysis for the formation of various carbon-carbon bond, a new era of research was achieved. Reactions like Heck, Suzuki, Sonogoshira, Negishi, Kumada, Stille, etc were discovered.[6] Transition metal-catalysed C-C bond has changed role in shaping chemical synthesis and opened a new era in synthetic chemistry. Although, several transition metals have been used for the formation of carbon bond for example, Ni, Cu, Fe, and Co, palladium-based catalysts comprise the most useful tools to mediate C-C bond. Palladium has the broadest scope due to its high selectivity, tunability and reactivity. Using a small amount of Pd can proceed the reactions due to the high turnover number (TON) and turnover frequency (TOF) of Pd metal.[7,8] The outstanding capability of palladium to construct C-C bonds between functionalized substrates has allowed the transformation of C-C bond that were previously unsuccessful or only possible using multi-step approach. The work of scientists in the 1970s laid the foundations for the technology of the coupling reactions. Their development and wide-ranging application became turbulent after the full realization of their synthetic usefulness and the discovery of metal complexes with bulky, strongly donating ligands. The popularity and success of this research field led to the awarding of the chemistry prize in 2010 to R. F. Yes, E. I. Negishi and A. Suzuki.[9] The Mizoroki-Heck reaction is a reaction that formed a carbon-carbon bond between

an organic halide, vinyl halide or benzylhalide and an alkene in the presence of a palladium catalyst and a base to form a substituted alkene as shown in Figure 1-1. The reaction was discovered by Mizoroki and Heck in 1971 and 1972, respectively, through independent research.[10] Among basic types of C-C cross-coupling reactions, Heck reaction has received considerable attention in synthetic organic chemistry due to high efficiency and simplicity.

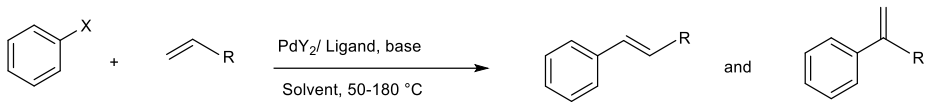

X= I, Br, Cl, COCl, OSO_2R, SO_2Cl, $C(O)OC(O)Ar$,SiR_2OH

Y= Cl, OAc

Figure 1-1 Heck C-C cross coupling reaction condition

In the early 1970s, Heck[12] and Mizoroki[11] independently reported the coupling between an olefin and an organic halide in the presence of palladium which then was altered by changing the conditions. The varieties within the methods included the utilize of distinctive metal, ligands, or substrates.[13-17] The phosphine-ligated palladium complexes catalyzed coupling between a halides and terminal alkenes is considered to be the most important frequently employed method of preparing a substituted alkene in high reactivities and selectivites.[18-22] Heck C-C cross-coupling reactions are employed in a wide array of synthetic reactions. They have been used in the industrial field of homogeneous catalysts as shown below in Figure 1-2 is the preparation of octyl-4-methoxycinnamate (UVB sunscreen) that produces by the Dead Sea, via Heck C-C cross coupling reaction as the key step in its process.[23] In the reaction below the first step is the brominated of methoxybenzene in the para-position with 97% selectivity. Then, the reaction of p-bromoanisole with octyl acrylate is carried out with octyl acrylate to produces octyl-4-methoxycinnamate.

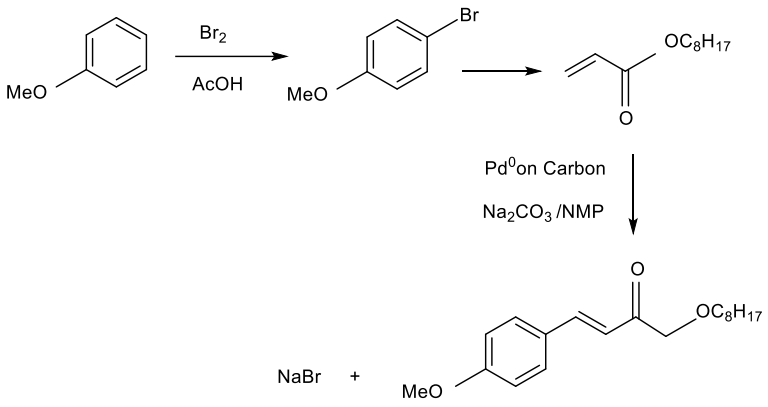

Figure 1-2 Heck C-C cross-coupling reactions in construction of octyl-4-methoxycinnamate

The formation of Naproxen is another example of the use of Heck C-C cross-coupling reactions. Naproxen is a generic analgesic that was discovered by Albemarle as shown below in Figure 1-3. In the production of Naproxen, reaction between 2-bromo-6-methoxynaphthalene and ethylene takes place which then a carbonylation of the product gives the Naproxen.

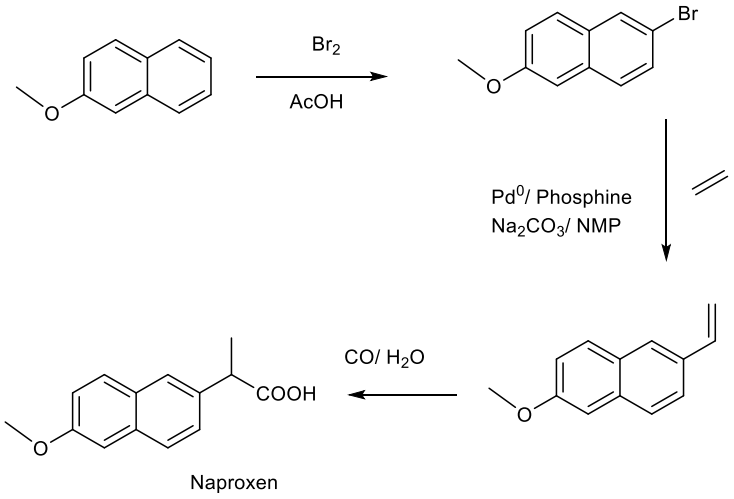

Figure 1-3 Heck C-C cross-coupling reaction usage in construction of Naproxen

Heck C-C cross-coupling reaction has been also used for electronic components as shown in Figure 1-4. The production of benzocyclobutene which known as Cyclotene is one example of the use of Heck C-C cross-coupling reaction for electronic components.[24]

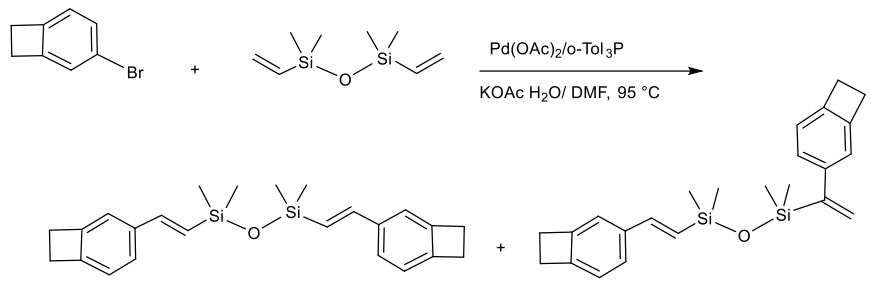

Figure 1-4 Use of Heck C-C cross-coupling reactions in electronic components

Singulair is a medicine that used to prevent asthma attacks by blocking the activities of leukotriene. Heck C-C cross-coupling reaction is used in one of few steps to synthesize the Singulair complex, as shown in Figure 1-5.[24]

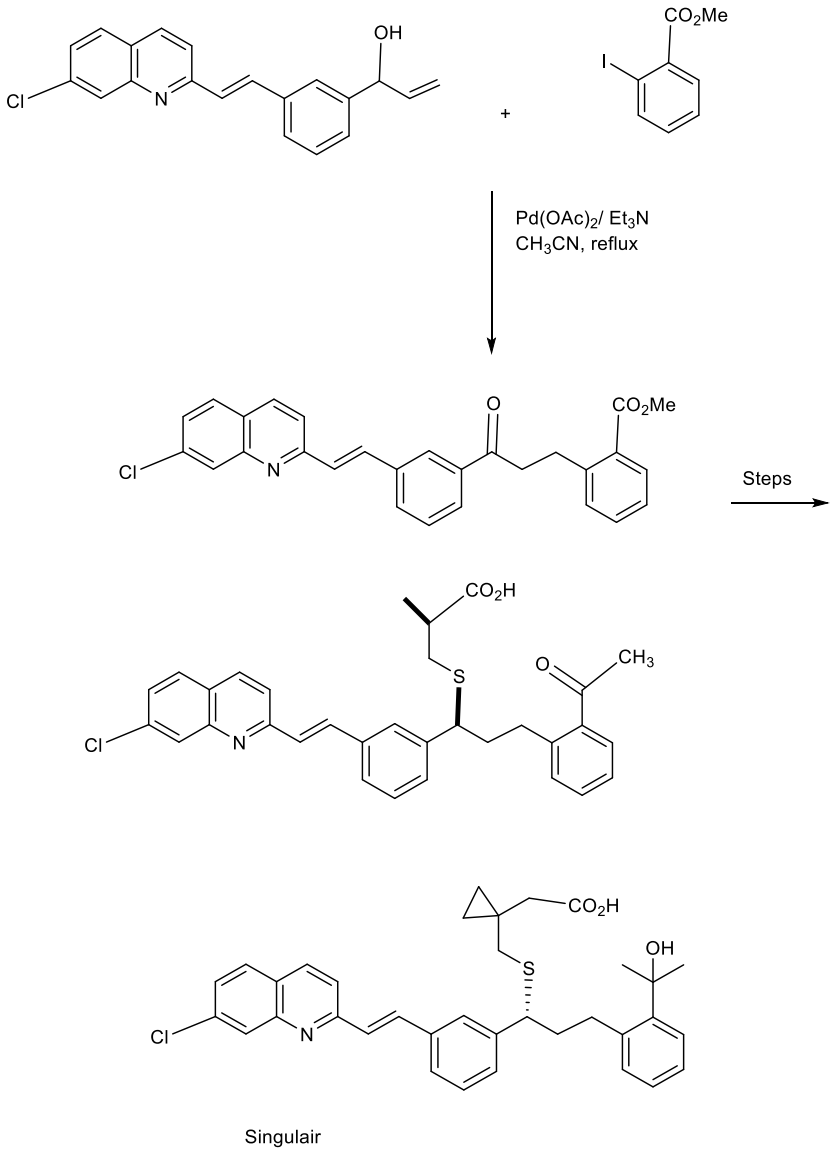

Figure 1-5 The usage of Heck C-C cross-coupling reaction in the synthesis of Singulair

1.1.2 Mechanistic considerations

The mechanism of Pd-catalyzed Heck C-C cross-coupling reaction is shown in Figure 1-6. The mechanism involves the pre-activation of palladium catalyst, oxidation addition, coordination-insertion, β-hydride elimination-d, and regenerating of the active catalyst species.

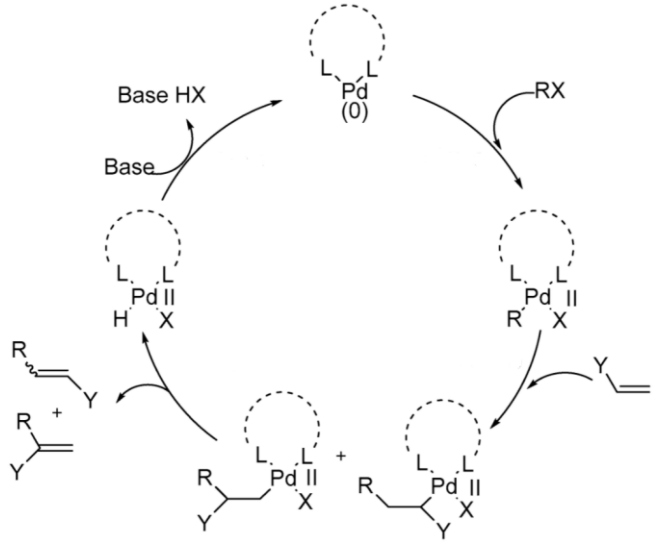

Figure 1-6 A generally accepted reaction mechanism for Heck C-C cross-coupling reaction [26]

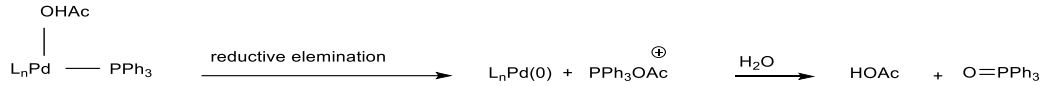

Figure 1-7 Reductive elimination of Pd (II) to Pd (0)

Pre-activation of Palladium catalyst

The cycle is beginning with the activation of the catalyst. In this step Palladium (ll) is reduced to [Pd (0)L_2]. Monodentate phosphine ligands such as PPh_3 are the most popular ligands used to catalyze the reaction, and the reduction is promoted as shown in Figure 1-7.[26]

Oxidative addition

In this step which it is considered to be the most difficult step, the aryl or vinyl halide undergoes oxidative addition. The palladium is oxidized from 0 to +2. PdL_2 is the coordinately unsaturated, which means it is electron-rich, nucleophilic, and has vacant sites, allowing for the oxidative addition of organic electrophile to produce trans-RPdXL2.[26]

Coordination-insertion

After the formation of trans-$RPdXL_2$ in the previous step, the alkene is inserted as a syn to form a σ-alkyl–palladium (II). Then a syn position of the palladium and β-hydrogen takes place after a rotation around the C-C bond. [25,26]

β-Hydride elimination

The elimination of β-hydride is dependent on the position of the palladium and the β-hydrogen hydride, which requires the palladium to be syn-coplanar to the β-hydride. After that, the alkene and the inactive $HPdXL_2$ species are generated.[26] So, then the base quenched the hydrogen halide to regenerate the PdL_2 and close the cycle.[2]

1.2 Photocatalysts

1.2.1 Photochemistry and photocatalysts

The use of visible light to initiate organic reactions have been conducted over the past 100 Years. In 1912, Giacomo Ciamician was the first chemist who used visible light for conducting reactions. Since then, photochemistry and photocatalysis have been used broadly to facilitate synthesis of organic compounds. Several factors come together to make the use of visible light possible. The energy of visible light is less than UV irradiation which means instead of a highly reactive intermediate that are environmentally harmful and costly, visible light can be used. Moreover, the high energy photons that are produced by absorption of energy from the ultraviolet region can cause uncontrolled photodecomposition. Furthermore, the absence of the absorbance of visible light by organic compounds, which reduces the side reaction stemming from photochemical reactions performed with UV light of high energy.[27,28,29]

A characteristic of a photocatalyst is the absorption of light and that leads to the generation of a molecule that is electronically excited, which ends up acting as a

photoredox catalyst. This situation arises because of an electron being promoted to an elevated level of energy, where a grounded state singlet (S_0) moves to a state of singlet excitation.[30] The potency of many inorganics and organometallics of absorbing visible light to promote organic transformations have inspired organic chemists to pursuit towards new reactions using photocatalysts.[27] Photocatalysts have been divided into two main categories, which include organic photocatalysts and metal complexes. Several studies have examined organic photoredox catalysis as used in the field of chemistry. Transition metal catalysts-based catalysts have been used as a photoredox catalysts due to their abilities to absorb visible light. In addition, a variety of organic compounds are known to participate in synthetic transformations because of their versatility and capability to take part in photoinduced electron transfer, also known as PET.[31] The oxygenation of benzene to phenol is an example of an organic photocatalyst that used 2,3- dichloro-5,6-dicyano-p-benzoquinone (DDQ) as a photocatalyst. The conventional synthetic routes of phenol from benzene requires more than one step. The synthesis of phenol directly from benzene can be obtained by using heterogeneous inorganic catalysts. However, using these catalytic systems have the drawbacks of low yield, poor selectivity, and the need for high temperature. In contrast to inorganic catalysts, benzene can also be oxidized using DDQ as a photocatalyst with xenon lamp (500 W) illumination in an oxygen-saturated acetonitrile solution of benzene, with a yield of 99% of phenol and 99% conversion with >99% selectivity as demonstrate in Figure 1-8.[32]

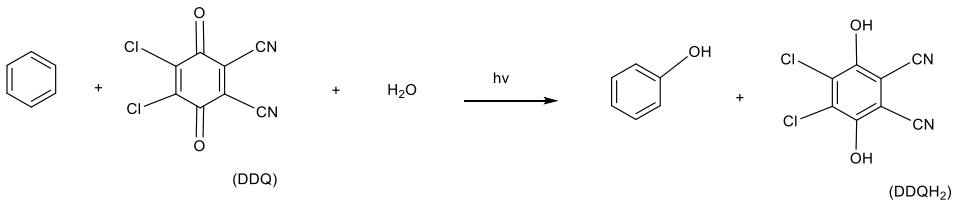

Figure 1-8 The oxygenation of benzene to phenol using DDQ as a photocatalyst

There are numerous studies conducted in organic synthetic using inorganic photoredox catalysts. One of the first examples was demonstrated by Cano-Yelo and Deronzier. The use of photoredox catalysis enabled the formation of phenanthrene carboxylic acid, which would otherwise yield a very low yield as shown in Figure 1-9.

Stilbene diazonium ion undergoes an intramolecular arylation after being exposed to visible light in the presence of $[Ru(bpy)3]^{2+}$ in acetonitrile to construct phenanthrene carboxylic acid with 100 % yield.[3]

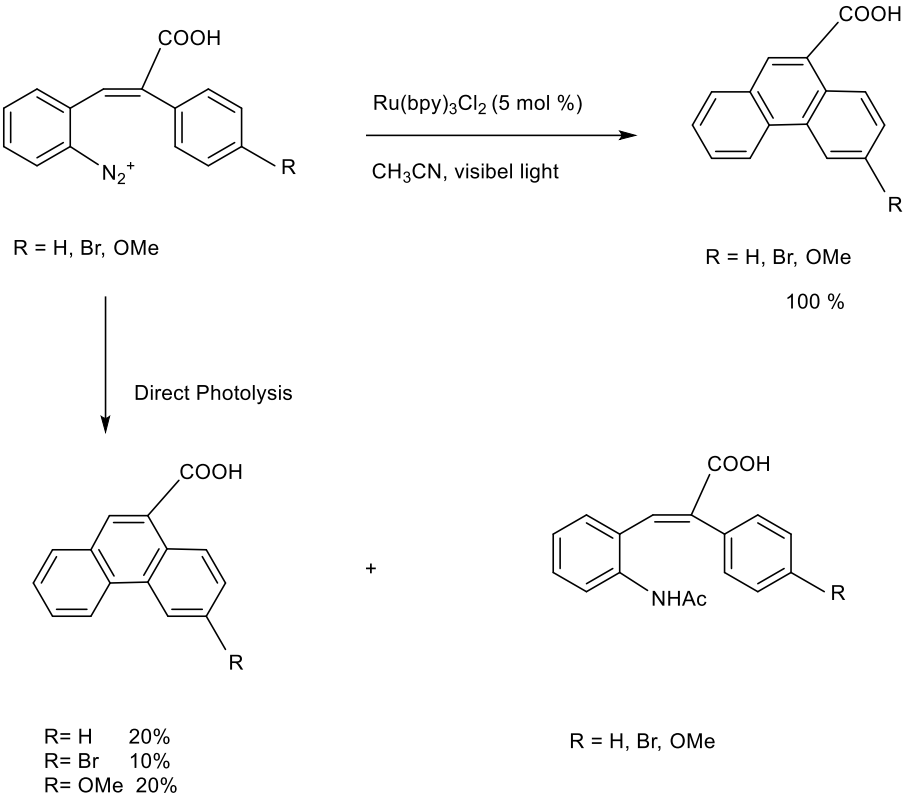

Figure 1-9 Formation of phenanthrene carboxylic acid using $[Ru(bpy)3]^{2+}$ as a photocatalyst

1.2.2 Mechanisms of photocatalysis

1.2.2.1 Photoredox catalysis

The process of photoredox catalysis derives from various reactions, including the one involving photoredox catalysis is distinguished as catalytic organic reactions, including the one involving a single electron transfer through a radical intermediate. Several mechanistic aspects of the process of photoredox catalysis have been suggested in numerous studies. The key findings of these studies on the photophysics process indicate that the absorption of light leads to the generation of a molecule that is electronically excited, which end up acting as photoredox catalyst. This situation arises because of an electron being promoted to an elevated level of energy, where a grounded state singlet (S_0) moves to a state of singlet excitation. When the catalyste gets excited, that generated a stable state for long time which allows the electron to transfer to another molecule. These complexes, however, are weak oxidants and reductants before irradiation, they become very potent in their exited state in transferring energy to another substance. Photoredox catalysis can be explained with the example of $[Ru(bpy)_3]^{+2}$. A long-lived excited state was created by the irradiation of the complex which resulted in the transfer of an electron from the metal-centered t_{2g} orbitals to the ligand-centered. This is referred to as a charge transfer from metal to ligand. As a result, in a Ru (II) has been converted to a Ru (III). The ligand undergoes a single-electron reduction. The excited state rapidly undergoes intersystem crossing to form the lowest-energy triplet state. The exited state has a longer lifetime due to the fact that the exited state is a triplet and the ground state is a singlet which is a forbidden transition and therefore, often slow.

Relative to the ground state species, photoexcited species has both stronger oxidizing and reducing properties. By using standard reduction potentials this phenomenon can be demonstrated.

$Ru(bpy)_3^{3+} + e^- \rightarrow {}^*Ru(bpy)_3^{2+}$ $\quad E_{1/2}{}^{III/*II} = -0.81$ V vs SCE

$Ru(bpy)_3^{3+} + e^- \rightarrow Ru(bpy)_3^{2+}$ $\quad E_{1/2}{}^{III/II} = +1.29$ V vs SCE

The excited complex $^*Ru(bpy)_3^{2+}$ is a more potent reducing agent than the unexcited complex. The reduction potential of excited state $E_{1/2}{}^{*II/I} = +0.77$ V vs SCE species is more potent than the ground state $E_{1/2}{}^{II/I} = -1.33$ V vs SCE. There are two ways that can happen involving oxidation or reduction of the excited state as shown in Figure 1-10. When the photocatalyst acts as a reductant, it can generate a high energy electron, which can easily be donated to another molecule. The vacant site that has been generated can act as a hole and accept electron.[34]

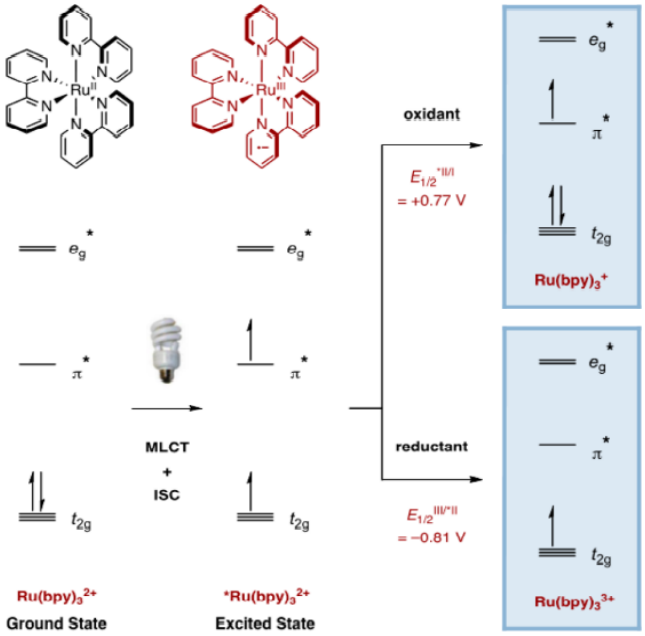

Figure 1-10 photochemical properties of $(Ru(bpy)3]^{2+}$

1.2.2.2 Energy transfer

SET process cannot be applied in all organic molecules because many of these compounds have oxidation or reduction potentials that are incompatible with the excited photocatalysts. Visible-light-induced reactions can also occur through EnT

processes considering the relatively high energy of the triplet state of the excited photocatalyst which can serve as an energy donor that transfer energy to the substrate which serve as an energy acceptor. First, by irradiation with visible light, the photocatalyst will be excited into higher energy orbital S_1. Then an intersystem crossing prosecco is taking place to produce the photocatalyst in its lowest energy triplet state which facilitate the transferred of the energy to the substrate. This will cause the substrate to be excited.[35] Dexter energy transfer is the most common mechanism that explains the EnT process in photocatalysis Figure 1-11. For an efficient transfer of energy, the donor triplet must be higher in energy than that of the acceptor. The process has to be also thermodynamically feasible.[36]

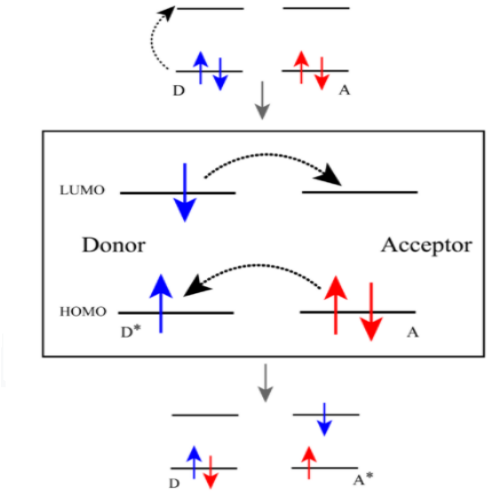

Figure 1-11 Dexter energy transfer process

Over the last decade, the EnT strategy has impacted the area of synthetic of photochemistry significantly, with several successful transformations developed by various research groups. $Ru(dtbbpy)_3(PF_6)_2$ was used by Farney and Yoon as a photocatalyst to produce pyrroles and indoles. The catalysis is suggested to proceed through an EnT process. The authors proposed the following mechanism. First, the excited-state of the photocatalyst generated with irradiation with visible-light. Then, the energy can be transferred to the vinyl azide and excited the substrate. Consequently,

one nitrogen molecule is released from the triplet state of vinyl azide resulting in a nitrene intermediate. Then, a cyclization of the product form azirine compound. Finally, an intramolecular cycloaddition of azirine is carried out to give the pyrrole as shown Figure 1-12.[35]

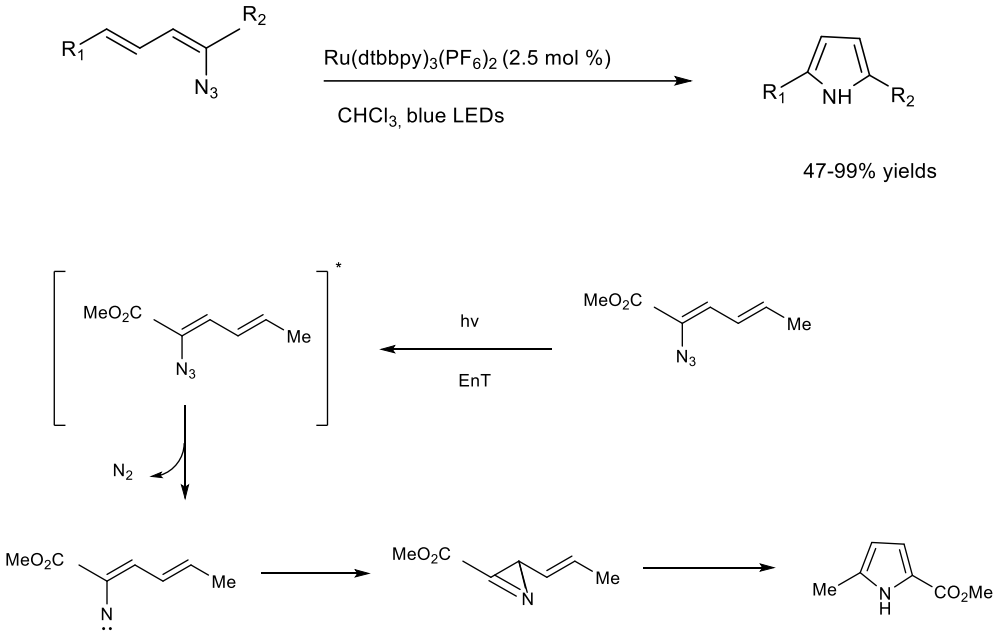

Figure 1-12 Synthesis of pyrroles by intramolecular cycloaddition of vinyl azides

The E to Z isomerization of alkenes is not readily accessible due to (Z)-alkenes being unstable. Although the chemists have utilized UV light in the isomerization of carbon–carbon double bonds for long time, its applicability is limited because of the highly energetic UV light.

Osawa et al. described a visible-light-induced rection using a polypyridine ruthenium (II) complex ([CpRu(CH_3CN)(CO)(Pru)]($PF6)_3$) as the photocatalyst to promote the E to Z isomerization of 4-cyanostilbene. Proposed mechanism suggested that an energy transfer from excited photocatalyst to the 4-cyanostilbene substrate to give Z alkene from E alkene as shown Figure 1-13.[35]

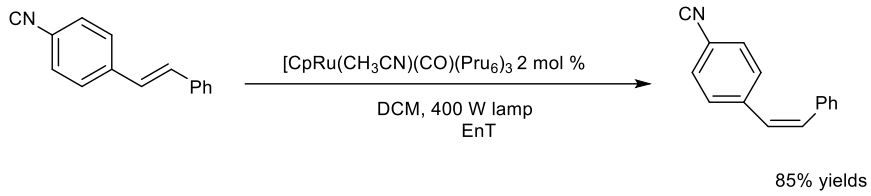

Figure 1-13 E to Z alkene isomerization through an EnT process

1.3 BODIPY

1.3.1 Characteristics of BODIPY

In 1968, BODIPY was discovered by Treibs and Kreuzer as an important class of fluorescent dyes .[37] BODIPY has attracted much interest in recent years for being fluorescent dyes with unique characteristics, which have made these chromophores to be used in a large scale in many different fields, such as, analytical chemistry, biological in vivo imaging, solar cells, biology, medicine, photosensitizers, and photocatalysis.[38,39] BODIPY dyes strongly robustness toward light. [40]

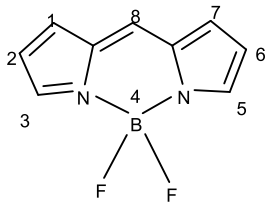

Figure 1-14 The core structure of BODIPY and its numbering

1.3.2 BODIPY in photoredox catalysis

Photocatalysts that are triplet photosensitizers, such as $Ru(bpy)_3Cl_2$, are commonly used. However, when compared to BODIPY, transition metal complexes have lower absorption of visible light ($\varepsilon < 20{,}000\ M^{-1}\ cm^{-1}$) at 450 nm, whereas BODIPY dyes have

high visible light absorption (40 000-110 000 M^{-1} cm^{-1}). Moreover, the triplet state lifetime of these photosensitizers is short (τT = 0.89 μs).

The photocatalyst and substrate molecules benefit from the photocatalysts being strangely absorbing visible light. As a result, BODIPY-based catalysts are widely used in phot redox catalysis. Jianzhang Zhao and his group have used C_{60}-Bodipy dyes as photoredox catalytic.

The synthesis of bioactive pyrrolo[2,1-a] isoquinoline was carried out with BODIPY-C_{6o}. C_{60} is known as an electron acceptor but it shows week absorption of visible light itself. C_{60}-Bodipy conjugates show a strong absorption of light as well as a long-lived triplet excited state that can be generated upon excitation. The synthesis of bioactive pyrrolo[2,1-a] isoquinoline was synthesized in the presence of BODIPY-C_{6o}. A yield of 91% was obtained when C_{60}-Bodipy was used while 37% was obtained when [$Ru(bpy)_3Cl_2$] was used.[42,43]

BODIPY dyes have been also used in photocatalyst by our group in a previous work. In which BODIPY- functionalized palladium (II) complex was utilized as an effective photoredox catalyst for the Sonogashira C-C cross-coupling reactions in the presence of visible light as shown in Figure 1-15. A higher yield was achieved when BODIPY- functionalized palladium (II) complex was used, than from the conventional method. BODIPY's role in this catalytic mechanism is to absorb light and transfer energy to the palladium. It was found that in the absence of the BODIPY the yield drops dramatically from 92% to 17% indicating the importance of BODIPY. Furthermore, low yield was observed in the absence of light, confirming that BODIPY plays an important role in catalysis.[44]

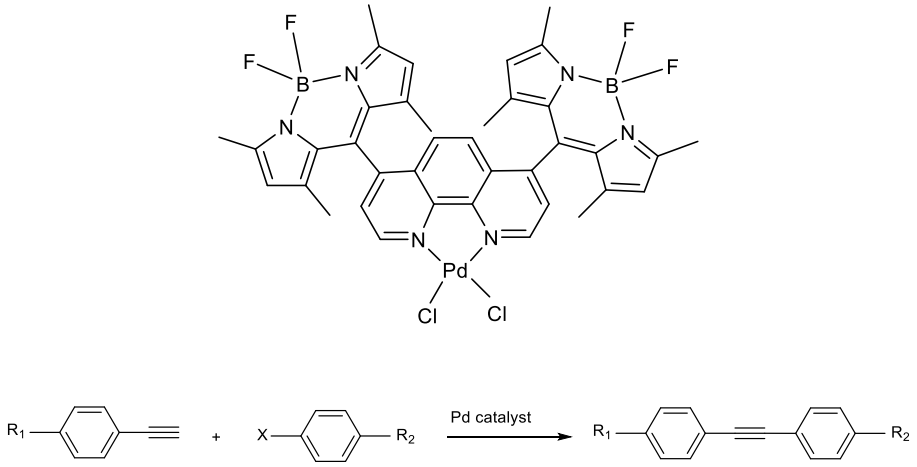

Figure 1-15 Sonogashira C-C cross-coupling reactions and the palladium catalysts used in the study

1.4 Objectives

Goals of this research was to:

1. Synthesize of three BODIPY based Py-BODIPY-Pd catalysts.
2. Use UV-Vis spectroscopy, ^{1}H NMR, and fluorescence spectroscopy to characterize the products and intermediates.
3. Use the three catalysts for Heck C-C cross-coupling reactions.
4. Examine the effect of substitutes on product yield

2 Experimental

2.1 General information

The complexes' synthesis procedure is described below. All starting reagents and materials (Sigma-Aldrich, Alfa Aser) are commercially available. Bruker Avance II-NMR spectrometer at 400 MHz in $CDCl_3$ with tetramethylsilane (TMS) as a standard was used to record ^{1}H NMR spectra. A Dual Beam Cary 100 UV/vis spectrometer was used to record UV/vis absorption spectra. Fluorescence spectra were collected using an Edinburgh Instruments Spectro fluorometer FS5. VTI Glovebox was used to perform Heck C-C cross-coupling reactions under inert gas conditions.

2.2 Synthesis

2.2.1 Synthesis of (4 ',4 "-difluoro- 1 ',3 ',5 ', 7'-tetramethyl-4 '-bora-3 'a,4 ' diaza-s-indacene)- 4-pyridine

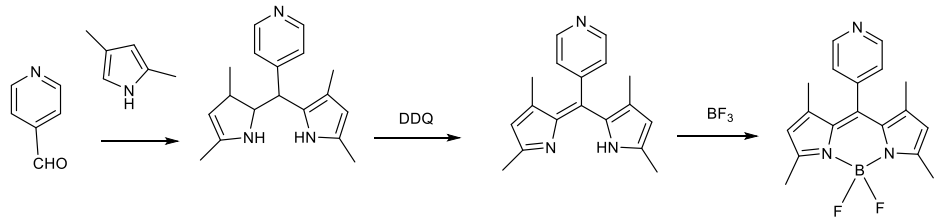

Figure 2-1 Synthesis of 4-Py-BDP ligand

To a 250 mL two-neck flask was added of dimethyl pyrrole (0.38 g, 4.0 mmol) and of 4-pyridinecarboxaldehyde (0.21g, 2.0 mmol) in DCM under N_2. After 30 minutes several drops of trifluoroacetic acid were added to the mixture to initiate the reaction. The reaction was carried out under dark for 18 h at room temperature. Then dichloro dicyano benzoquinone (DDQ) (0.45 g, 2.0 mmol) was dissolved in 10 mL of dichloromethane and added to the reaction mixture. After approximately 5 hours of stirring, triethylamine (4.0 ml, 29 mmol) and BF_3OEt_2 (4.0 ml, 31 mmol) of were added sequentially. After about 30 min of stirring the solvent was removed by evaporation, and the crude product was loaded on the column for purification using DCM/MeOH (v:v, 100:2) as an elute. This yielded an orange solid (0.088 g, 12 %).

^{1}H NMR (400 MHz, $CDCl_3$) δ: 8.764 (d, 2H), 7.288 (d, 2H), 5.988 (s, 1H) 2.541 (s, 3H), 1.388(s, 3H).

2.2.2 Synthesis of (4 ',4 "-difluoro- 1 ',3 ',5 ', 7'-tetramethyl-4 '-bora-3 'a,4 ' diaza-s-indacene)-3-pyridine

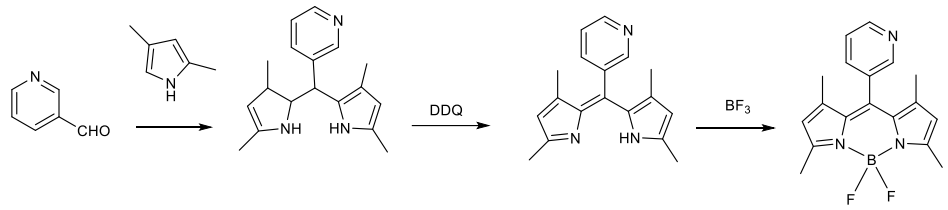

Figure 2-2 Synthesis of 3-Py-BDP ligand

The 3-Py-BODIPY ligand has been synthesized in the same way as for 4-Py-BODIPY ligand and the same amount of chemical reagents were used. The only difference is aldehyde substrate, instead of using 4-pyridinecarboxaldehyde, 3-pyridinecarboxaldehyde was used. The crude product was loaded on the column for purification using DCM/MeOH (v:v, 100:3) as an elute. This yielded an orange solid (0.124 g, 17%).

^{1}H NMR (400 MHz, $CDCl_3$) δ: 8.738 (d, 1H), 8.556 (s, 1H), 7.631 (d, 1H) 7.441 (t, 1H), 5.992 (s, 1H), 2.545 (s, 3H), 1.362 (s, 3H).

2.2.3 Synthesis of (4 ',4 "-difluoro- 1 ',3 ',5 ', 7'-tetramethyl-4 '-bora-3 'a,4 ' diaza-s-indacene) -2-pyridine

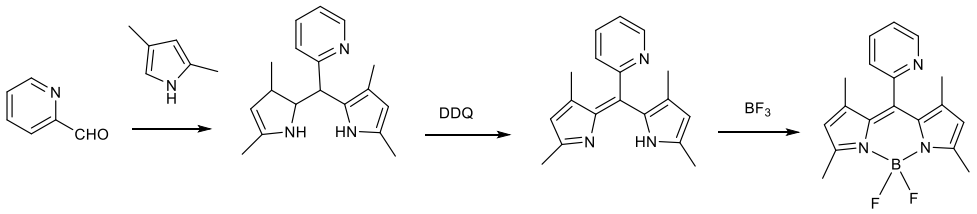

Figure 2-3 Synthesis of 2-Py-BDP ligand

The 2-Py-BODIPY ligand has been synthesized in the same way as 4-Py-BODIPY ligand and the same amount of chemical reagents were used. The only difference is aldehyde substrate, instead of using 4-pyridinecarboxaldehyde, 2-pyridinecarboxaldehyde was used. The crude product was loaded on the column for purification using DCM/MeOH (v:v, 100:3) as an elute. This yielded an orange solid (0.126 g, 18%).

^{1}H NMR (400 MHz, $CDCl_3$) δ: 8.761 (d, 1H), 7.815 (t, 1H), 7.414 (t, 1H), 5.961 (s, 1H), 2.535 (s, 3H), 1.293 (s, 3H).

2.2.4 Synthesis of dichloro (4 ',4 "-difluoro- 1 ',3 ',5 ', 7' -tetramethyl-4 '-bora3 'a,4 'a-diaza-s-indacene)- 4-pyridine) palladium (II) (4-Py-BODIPY-Pd)

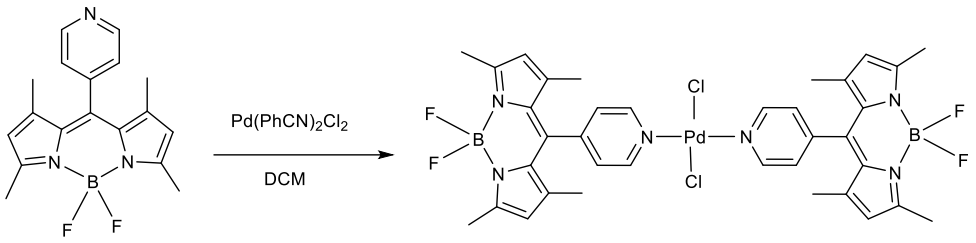

Figure 2-4 Synthesis of 4-Py-BDP-Pd catalyst

To 250 ml RBF, (0.029 g, 0.07 mmol) of $[PdCl_2(NCPh)_2]$ was weighed out and dissolved in 40 m l of $CHCl_3$. After $[PdCl_2(NCPh)_2]$ was completely dissolved in the solvent (0.053 g, 0.15 mmol) of 4-Py-BDP was weighed out and added to the mixture. The mixture was stirred for 3 hours in the dark. The solvent was removed from the product after completion of the reaction, and the purification was done using column chromatography with DCM/MeOH (v:v, 100:3). This resulted in an orange solid (0.086 g, 65%).

^{1}H NMR (400 MHz, $CDCl_3$) δ: 9.027(d, 2H), 7.386 (d, 2H), 6.03 (s, 1H) 2.547 (s, 3H), 1.408 (s, 3H)

2.2.5 Synthesis of dichloro (4 ',4 "-difluoro- 1 ',3 ',5 ', 7' -tetramethyl-4 '-bora3 'a,4 'a-diaza-s-inacene)- 3-Pyriden) palladium (II) (3-Py-BODIPY-Pd)

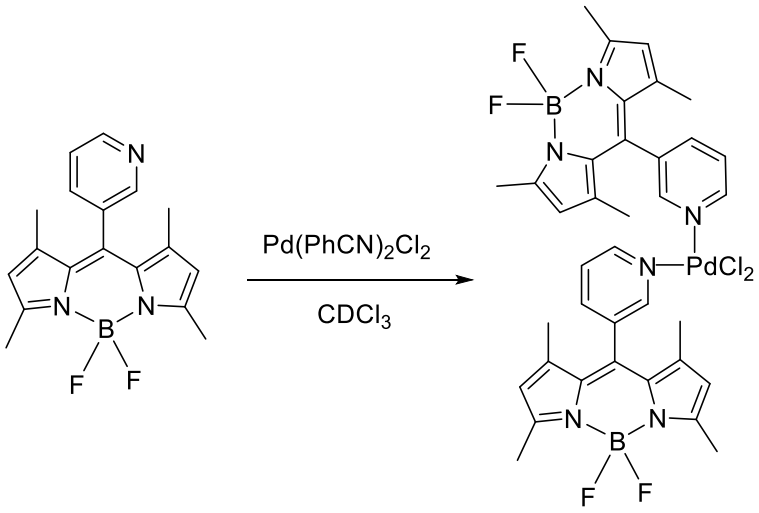

Figure 2-5 Synthesis of 3-Py-BDP-Pd catalyst

To 250 ml RBF, (0.038 g, 0.10 mmol) of $[PdCl_2(NCPh)_2]$ was weighed out and dissolved in 40 ml of $CHCl_3$. After $[PdCl_2(NCPh)_2]$ was completely dissolved in the solvent (0.123 g, 0.20 mmol) of 3-Py-BDP was weighed out and added to the mixture. The mixture was stirred for 3 hours in the dark. The solvent was removed from the product after completion of the reaction, and the purification was done using column chromatography with DCM/MeOH (v:v, 100:3). This yielded an orange solid (0.134 g, 88%).

^{1}H NMR (400 MHz, $CDCl_3$) δ: 8.935 (d, 1H), 8.836 (s, 1H), 7.752 (d, 1H) 7.487 (t, 1H), 5.989 (s, 1H), 2.528 (s, 3H), 1.401 (s, 3H).

2.2.6 Synthesis of dichloro (4 ',4 "-difluoro- 1 ',3 ',5 ', 7' -tetramethyl-4 '-bora3 'a,4 'a-diaza-s-indacene)- 2-Pyriden) palladium (II) (2-Py-BODIPY-Pd)

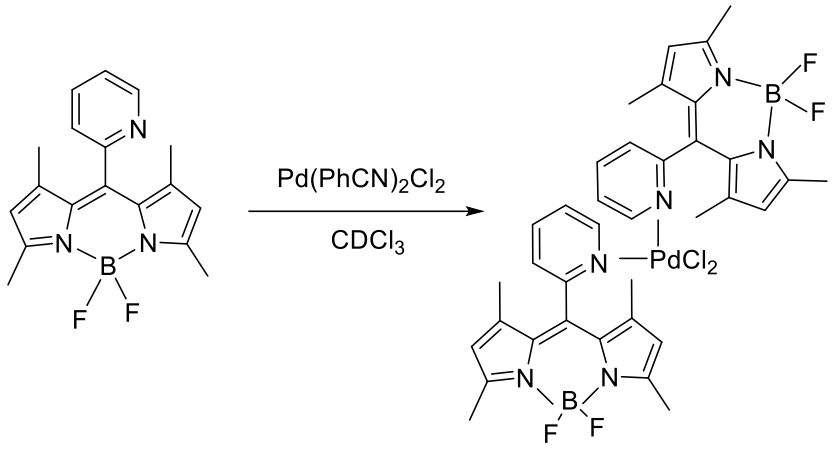

Figure 2-6 Synthesis of 2-Py-BDP-Pd catalyst

To 250 ml RBF, (0.096 g, 0.25 mmol) of $[PdCl_2(NCPh)_2]$ was weighed out and dissolved in 40 ml of $CHCl_3$. After $[PdCl_2(NCPh)_2]$ was completely dissolved in the solvent (0.163 g, 0.50 mmol) of 2-Py-BDP was weighed out and added to the mixture. The mixture was stirred for 3 hours in the dark. The solvent was removed from the product after completion of the reaction, and the purification was done using column chromatography with DCM/MeOH (v:v, 100:3). This yielded an orange solid (0.187 g, 92 %).

^{1}H NMR (400 MHz, $CDCl_3$) δ: 8.769 (d, 1H), 8.301 (s, 1H), 7.992 (t, 1H), 7.624 (t, 1H), 6.185 (s, 1H), 2.489(s, 3H), 1.245(s, 3H).

2.3 Heck C-C cross-coupling reactions

1. Reaction setup

The glove box was used to perform all reactions in an argon atmosphere. K_2CO_3 base (0.138 g, 1.00) mmol was added to the vial followed by Py-BODIPY-$PdCl_2$ catalyst (2.00 mg, 0.003 mmol). Then 2.00 ml of DMF, 45 µL, (0.50) mmol of methyl acrylate, and 61 µL, (0.50 mmol) of iodobenzene were added to the vial syringes sequentially to reaction mixture. Then, the reaction mixture was stirred for 24 hours. A 13W LED lamp was used for visible light irradiation.

2. Sample preparation for ^{1}H NMR analysis

The mixture of the reactions were studied using ^{1}H NMR spectroscopy in 0 and 24 hours. The internal reference was prepared by mixing 147 µL, (1.00 mmol) of trimethyl benzaldehyde in 4.00 ml of DMF solvent. The samples for NMR analysis at 0 h were prepared as follows. 50 µL of the reaction mixture was added to the NMR tube followed by 0.5 ml of $CDCl_3$ solvent. The samples for NMR analysis at 24 h were prepared as follows. 50 µL of the reaction mixture added to the NMR tube followed by 20 µL of the standard reference then 0.5 ml of $CDCl_3$ was added.

3. ^{1}H NMR analysis

Calculation

The method below was used to calculate yield % from ^{1}H NMR analysis. The moles of the product can be determined using the following equation:

$$m_B = m_R\left(\frac{\frac{I_B}{n_B}}{\frac{I_R}{n_R}}\right)$$

$$m_B = mol\ of\ product$$

$m_R = \ moles\ of\ reference\ being\ added$

$n = corresponding\ No.of\ Hs$

$I_B = integration\ of\ product$

$I_R = integration\ of\ standard\ refernce$

Then yield can be calculated from the equation below

$$Yield\ \% = \frac{(m_B)}{(m_A)} \times 100\%$$

$m_A = \ moles\ of\ \ corresponding\ starting\ material$

Reaction conditions: 0.50 mol methyl acrylate, 0.50 mmol iodobenzaldehyde in 2.00 ml of DMF for the reaction. 50 µL of the reaction mixture and 20 µL in reference in 0.5 ml of $CDCl_3$ for ^1H NMR. Reference: 1.00 mmol of trimethyl benzaldehyde in 4.00 ml of DMF.

m_A = (0.50 mmol) (50/2000) =0.0125 mmol

m_R= (1.00 mmol) (20/4000) = 0.005 mmol

2.4 Spectral measurements

2.4.1 UV-Visible spectroscopic measurements

Characterization

Stock solutions of 2-py-BODIPY, 3-py-BODIPY, and 4-py-BODIPY ligands were prepared by adding 3 ml DCM to 3 mg of the ligands in 50 ml volumetric flasks. 29 µL of stock solutions of each ligand were diluted in 2.5 mL DCM to give 4.00×10^{-6} mol/L). The diluted solutions (4.00×10^{-6} mol/L) were used to obtain UV-VIS spectra. Stock

solutions of 2-py-BODIPY-$PdCl_2$, 3-py-BODIPY-$PdCl_2$, and 4-py-BODIPY-$PdCl_2$ complexes were prepared by adding 3 ml of DCM to 3 mg of the complexes in volumetric flasks.74 µL of stock solutions of each complex were diluted in 2.5 mL DCM to give (4.00×10^{-6} mol/L). The diluted solutions (4.00×10^{-6} mol/L) were used to obtain UV-VIS spectra.

2.4.2 Fluorescence spectra

Stock solutions of 2-py-BODIPY, 3-py-BODIPY, and 4-py-BODIPY ligands were prepared by mixing 3 ml DCM to 3 mg of the ligands in 50 ml volumetric flasks. 29 µL of stock solutions of each ligand were diluted in 2.5 mL DCM to give 4.00×10^{-6} mol/L. The diluted solutions (4.00×10^{-6} mol/L) were used to obtain UV-VIS spectra. Stock solutions of 2-py-BODIPY-$PdCl_2$, 3-py-BODIPY-$PdCl_2$, and 4-py-BODIPY-$PdCl_2$ complexes were prepared by adding 3 ml of DCM to 3 mg of the complexes in volumetric flasks. 74 µL of stock solutions of each complex were diluted in 2.5 mL DCM to give (4.00×10^{-6} mol/L). The diluted solutions (4.00×10^{-6} mol/L) were used to record UV-VIS spectra. Ligands emission spectra were collected while scanning through visible light rang with excitation of 375 nm. Ligands excitation spectra were recorded with excitation of 375 nm while scanning in the 400-700 nm range. Catalysts emission spectra were collected while scanning through visible light range at a fixed excitation wavelength of 371.40 nm. Excitation spectra were collected using emission wavelength of 600 nm while scanning in the 400-700 nm rang.

3 Results and discussion

3.1 Synthesis aspects

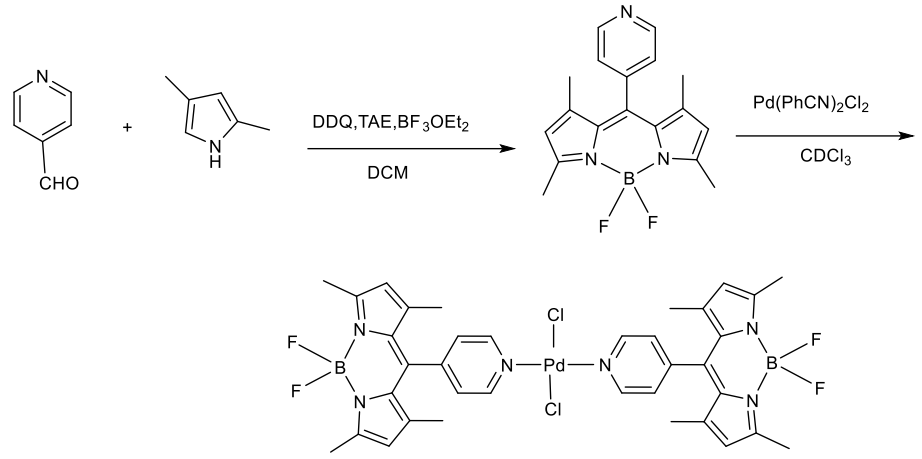

Figure 3-1 Synthesis of 4-Py-BODIPY-$PdCl_2$ catalyst

4-Py-BODIPY ligand was synthesized by reacting 4-pyridinecarboxaldehyde with dimethyl pyrrole in distilled DCM under N_2. To start the reaction, after 30 minutes a couple of drops of trifluoroacetic acid added to the reaction. To oxidize the carbon atom that connects two 2,4-diethylpyrroles and the pyridine moiety, DDQ was added to the reaction mixture. Eventually, $BF_3{\cdot}Et_2O$ was added to coordinate with two nitrogen atoms. The crude product was purified via column chromatography with DCM/MeOH (v:v, 100:3). This yielded an orange solid (0.1258 g ,18 %). The catalyst 4-py-BODIPY-Pd was synthesized from 4-Py-BODIPY ligand and $[Pd(PhCN)_2Cl_2]$ in a one-pot reaction. $[PdCl_2(NCPh)_2]$ was dissolved in $CHCl_3$ in a 250 mL RBF. After $[PdCl_2(NCPh)_2]$ was completely dissolved in the solvent, 4-Py-BODIPY was added to the mixture. After purification with column chromatography with DCM/MeOH (v:v, 100:3), this yielded an orange solid 65%.

3.2 Spectroscopic Characterization

3.2.1 ^{1}H NMR of 4-Py-BODIPY

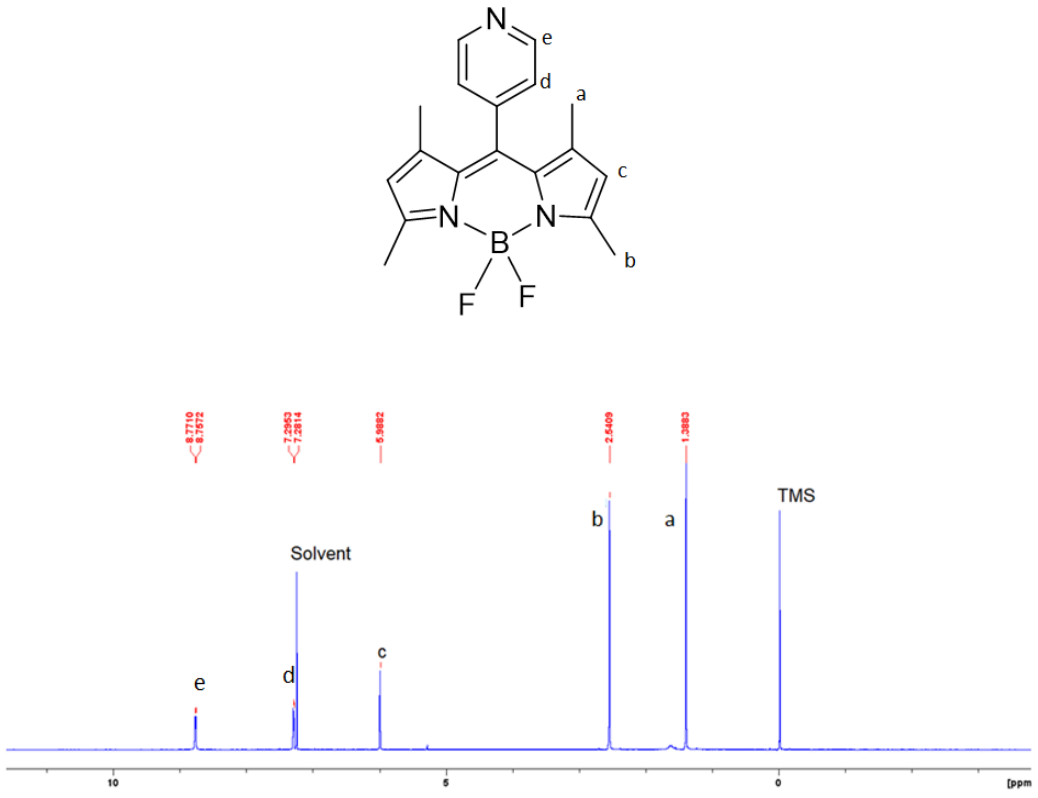

Figure 3-2 ^{1}H NMR spectrum of 4-Py-BDP in $CDCl_3$

Figure 3-2 shows the ^{1}H-NMR spectrum of 4-Py-BODIPY. There are two different aromatic protons in the pyridine ring appeared at the most de-shielded doublet peaks at 8.764 and 7.288 ppm. A singlet peak was observed at 5.988 ppm labelled as c, which correspond to the protons in the dimethyl pyrrole. The two methyl groups observed at 2.541 and 1.388 ppm as singlets labelled as a and b respectively.

3.2.2 ^{1}H NMR of 3-Py-BODIPY

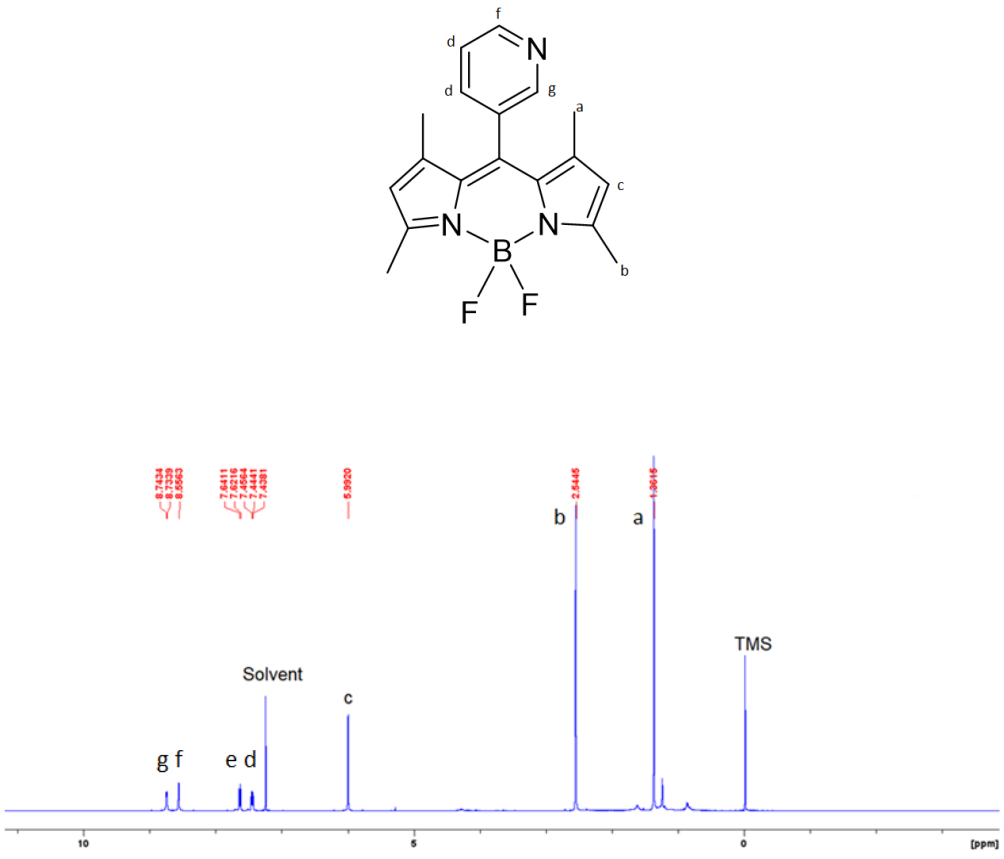

Figure 3-3 ^{1}H NMR spectrum of 3-Py-BDP in $CDCl_3$

Figure 3-3 shows the ^{1}H-NMR spectrum of 3-Py-BODIPY. There are four different aromatic protons appeared the most de-shielded peaks. The protons were observed at 8.738, 8.556, 7.631, 7.441 ppm. A singlet peak was observed at 5.992 ppm labelled as c, which correspond to the protons in the dimethyl pyrrole. The two methyl groups observed at 2.545 and 1.362 ppm as singlets labelled as a and b respectively.

3.2.3 ^{1}H NMR of 2-Py-BODIPY

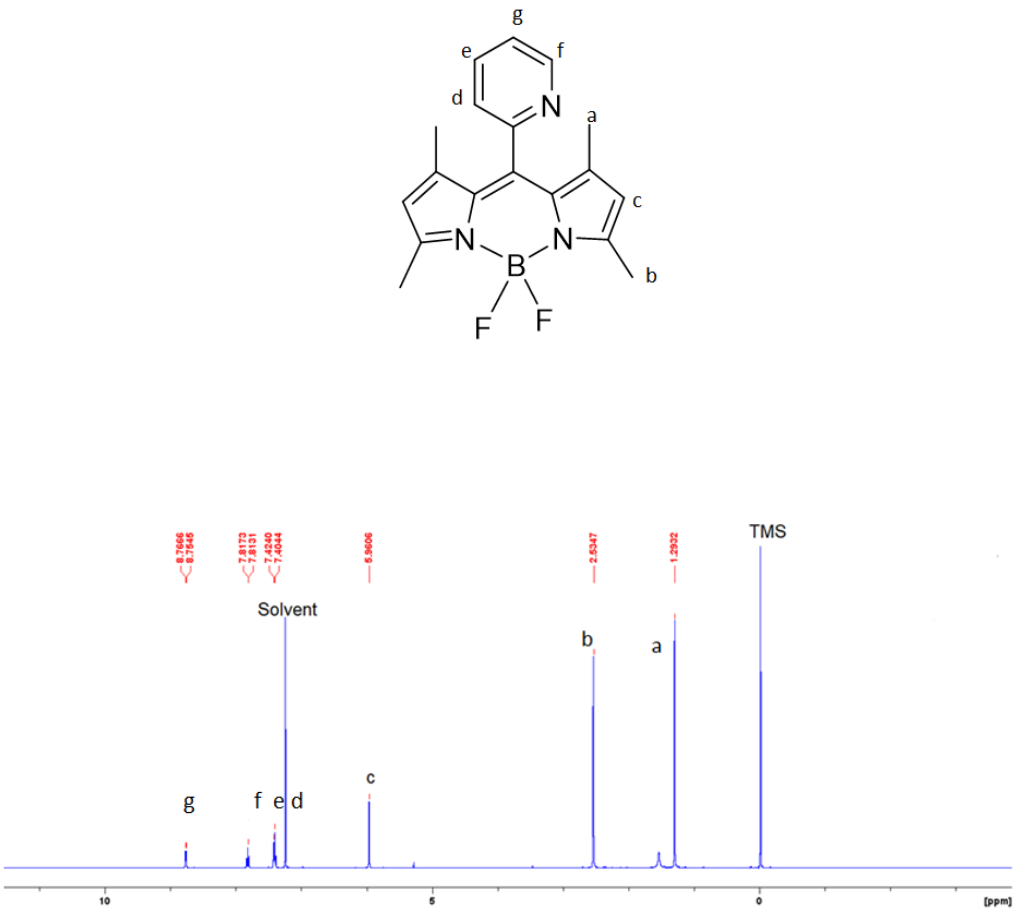

Figure 3-4 ^{1}H NMR spectrum of 2-Py-BDP in $CDCl_3$

Figure 3-4 shoes the ^{1}H-NMR spectrum of 2-Py-BODIPY. There are aromatic protons appeared the most de-shielded peaks. The protons were observed at 8.761, 7.815, 7.414 ppm. A singlet peak was observed at 5.961 ppm labelled as c, which correspond to the protons in the dimethyl pyrrole. The two methyl groups observed at 2.535 and 1.293 ppm as singlets labelled as a and b respectively.

3.2.4 ^{1}H NMR of 4-Py-BODIPY-Pd

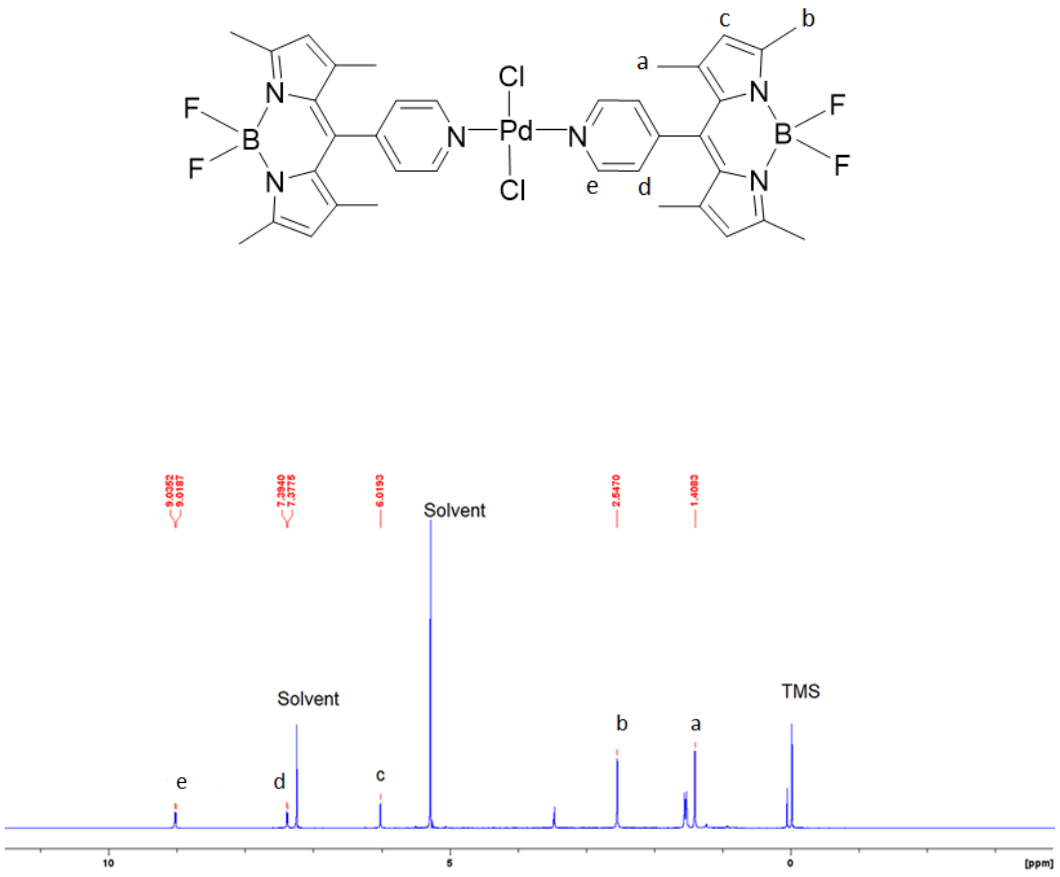

Figure 3-5 ^{1}H NMR spectrum of 4-Py-BD-Pd in $CDCl_3$

Figure 3-5 shows the ^{1}H-NMR spectrum of 4-Py-BODIPY-Pd. All the peaks that were observed for the ligand 4-Py-BODIPY were observed for the catalyst, except the two hydrogens attached to the pyridine ring which shifted more downfield.

3.2.5 ^{1}H NMR of 3-Py-BODIPY-Pd

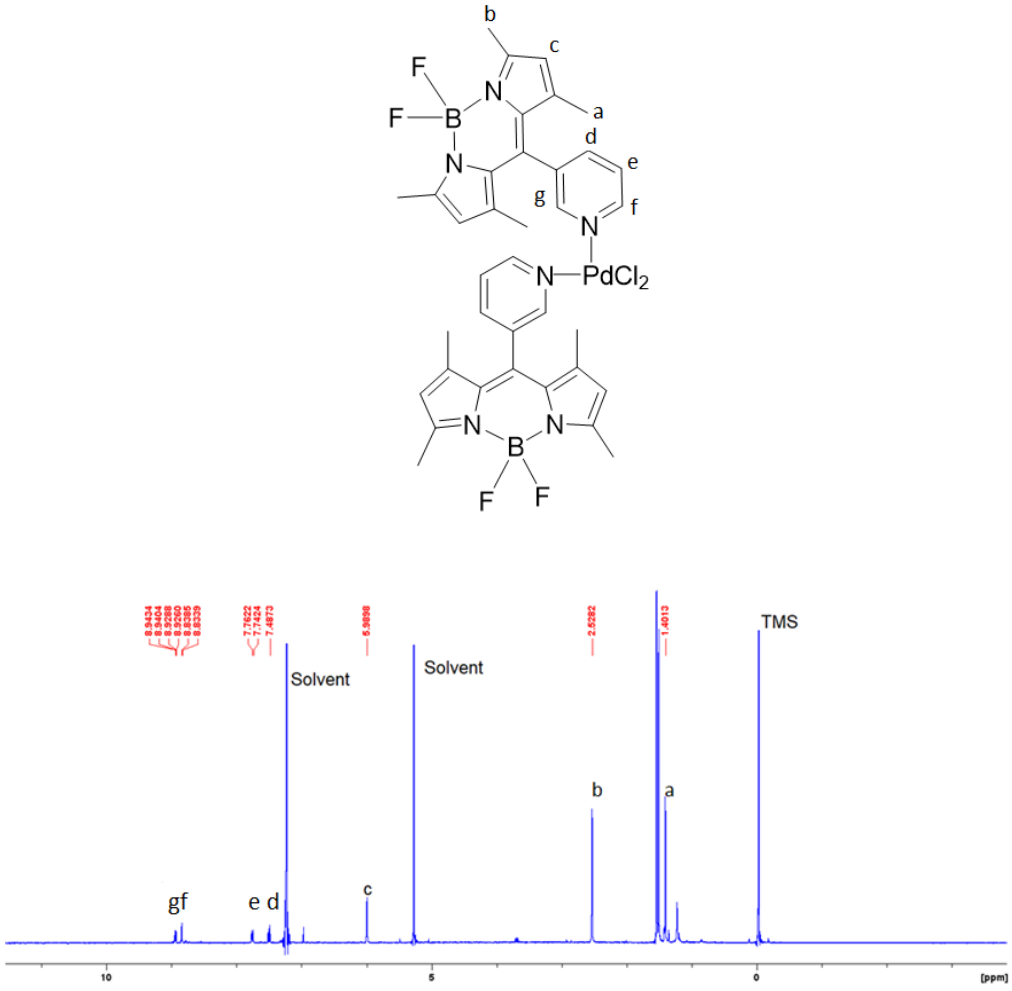

Figure 3-6 ^{1}H NMR spectrum of 3-Py-BDP-Pd in $CDCl_3$

Figure 3-6 shows the ^{1}H-NMR spectrum of 3-Py-BODIPY-Pd. All the peaks that were observed for the ligand 3-Py-BODIPY were observed in the catalyst, except the two hydrogens attached to the pyridine ring which shifted more downfield.

3.2.6 ^{1}H NMR of 2-Py-BODIPY-Pd

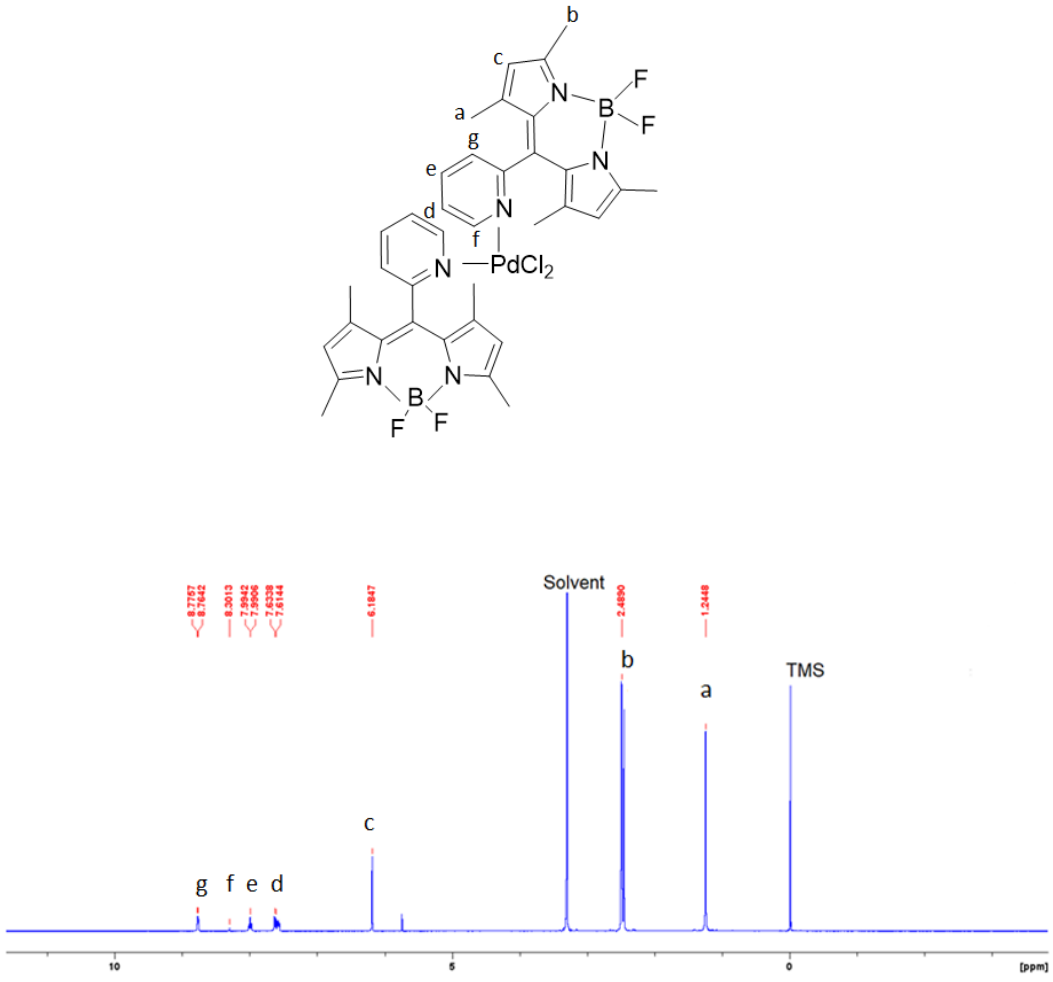

Figure 3-7 ^{1}H NMR spectrum of 2-Py-BDP in DMSO

Figure 3-7 shows the ^{1}H-NMR spectrum of 2-Py-BODIPY-Pd. All the peaks that were observed for the ligand 2-Py-BODIPY were observed in the catalyst, beside a singlet peak that appeared at 8.30 ppm that was not observed for the ligand which may overlapped with another peak.

3.3 UV-VIS spectroscopy

All the three ligands exhibit intense S_0–S_1 absorption bands in visible region between 400 nm to 700 nm as shown in Figure 3-8. 4-Py-BODIPY exhibit an absorption

maximum at 505 nm. Meanwhile, absorption maxima at 504 nm were observed for 3-Py-BODIPY and 2-Py-BODIPY.

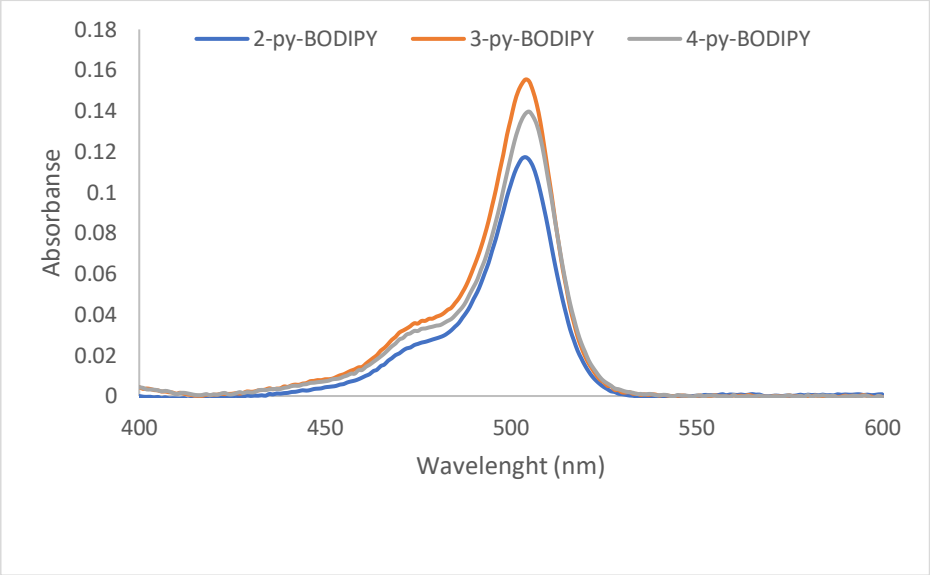

Figure 3-8 Absorption spectra for 4-Py-BDP, 3-Py-BDP, and 2-Py-BDP with a concentration of 4.0 x10^{-6}mol/L in DCM

It can be noticeable that after $PdCl_2$ being attachthe to the ligands, there is no significant change in terms of energy or position. As shown in Figure 3-9, complexes exhibit absorption bands in visible region between 400 nm to 700 nm. 4-Py-BODIPy-Pd exhibit an absorption maximum at 508 nm (ε = 1 .16 x 10^5 $M^{-1}cm^{-1}$) and 3-Py-BODIPY-Pd exhibit an absorption maximum at 507 nm (ε = 1 .36 x 10^5 $M^{-1}cm^{-1}$). Meanwhile, absorption maxima at 514 nm (ε = 4.92 x 10^4 $M^{-1}cm^{-1}$) was observed for 2-Py-BODIPY-Pd.

The Absorption coefficients $M^{-1}cm^{-1}$ were calculated by using Beer's Law equation.

$$A = \varepsilon lc$$

$$\varepsilon = A/lc$$

$$\varepsilon = \frac{0.467}{1\text{x}4.0\text{x}10^{-6}} = 1.16\text{x}10^{5} M^{-1} cm^{-1}$$

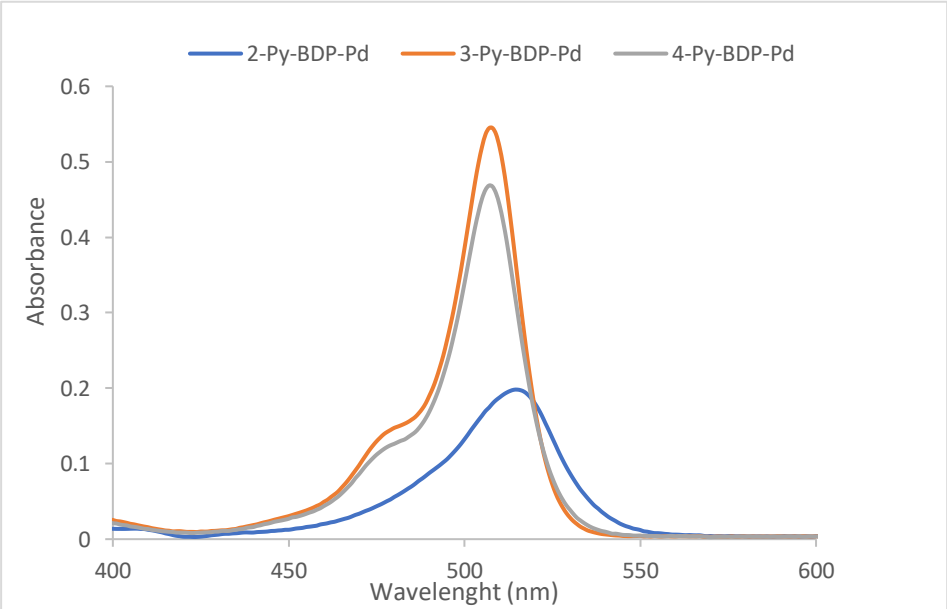

Figure 3-9 Absorption spectra for 4-Py-BDP-Pd, 3-Py-BDP-Pd, and 2-Py-BDP-Pd with a concentration of 4.0 x10^{-6} M in DCM

The energy absorbed by the catalyst is one of the most important features of an effective photocatalyst. The high absorption coefficient of the catalysts displays the quantity of energy that can be transferred to initiate the reaction. High absorption in the visible rang is exhibited by the catalysts and the high absorption coefficient are an indication of the effectiveness of the catalyst, with maximum absorption at 507, 508 and 514 nm. Also, the catalyst is critical in term of absorption light in the visible range, since organic substrates will not be activated using visible light.[52]

3.4 Fluorescence spectroscopy

The singlet fluorescence of 2-Py-BODIPY is observed at 518 nm, while fluorescence of both 3-Py-BODIPY and 4-Py-BODIPY is centered around 515 nm.

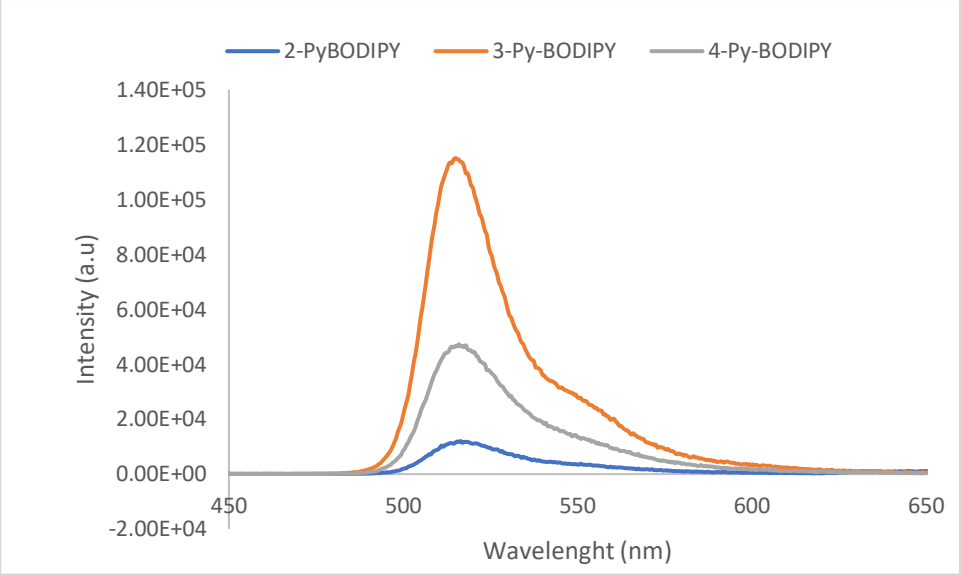

Figure 3-10 Fluorescence spectra for 4-Py-BDP, 3-Py-BDP, and 2-Py-BDP with a concentration of 4.0 x10^{-6} M in DCM

The longest wavelength of the emission maximum 535 nm was observed for 4-Py-BODIPY-Pd, while emission maxima at 520, 515 nm were observed for 3-Py-BODIPY-Pd and 2-Py-BODIPy-Pd, respectively.

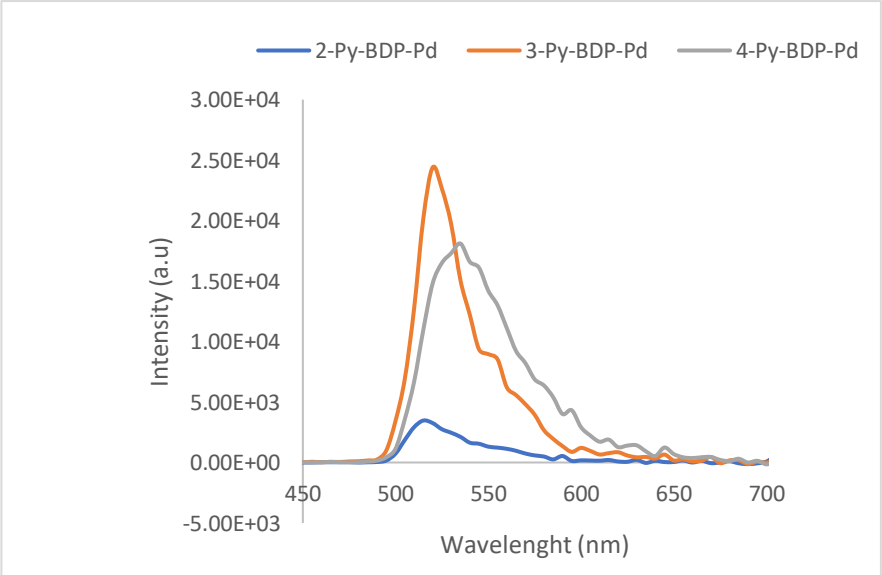

Figure 3-11 Fluorescence spectra for 4-Py-BDP-Pd, 3-Py-BDP-Pd, and 2-Py-BDP-Pd with a concentration of 4.0 x10^{-6} M in DCM

It should be pointed out that the attachment of Pd metal to the ligands reduced the fluorescence intensity drastically. One way to quench the fluorescence is by the heavy atom, but since Palladium and BODIPY are directly connected to the heavy atom effect is negligible. Some studies, however, tested the florescence in similar BODIPYs and proposed the charge separation process as an explanation for the quenching.[53]

Table 3-1 Spectra properties of ligands in DCM solvent

Ligand	Mass g/mol	Concentration M	Absorption nm	Fluorescence nm	Absorption coefficients $M^{-1}cm^{-1}$
4-Py-BDP	355.24	4.0×10^{-6}	505	515	3.4×10^{4}
3-Py-BDP	355.24	4.0×10^{-6}	504	515	3.8×10^{4}
2-Py-BDP	355.24	4.0×10^{-6}	504	518	2.9×10^{4}

Table 3-2 Spectra properties of complexes in DCM solvent

Complex	Mass g/mol	Concentration M	Absorption nm	Fluorescence nm	Absorption coefficients $M^{-1}cm^{-1}$
4-Py-BDP-Pd	932.90	4.0×10^{-6}	508	535	1.16×10^{5}
3-Py-BDP-Pd	932.90	4.0×10^{-6}	507	520	1.36×10^{5}
2-Py-BDP-Pd	932.90	4.0×10^{-6}	514	515	4.92×10^{4}

3.5 Heck C-C cross-coupling reactions

3.5.1 C-C cross-coupling reaction between iodobenzene and methyl acrylate

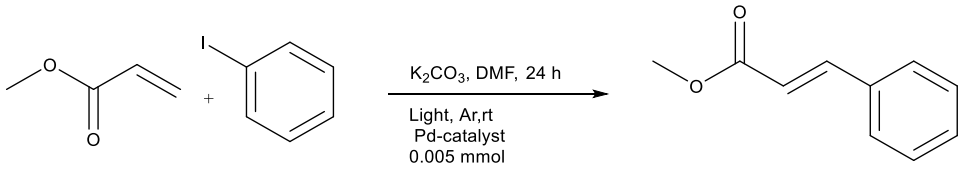

Heck C-C cross-coupling reaction is a reaction that producing a carbon-carbon bond between an aryl halide and an alkene that react in the presence of a palladium catalyst and a base to form a substituted alkene. The reaction conditions used in Heck C-C cross-coupling reaction involves DMF as the solvent, K_2CO_3 as a base, and ranging temperatures from room temperature to 180 °C. This condition is the most important frequently employed method of preparing a substituted alkene in high reactivities and selectivites. Hence, K_2CO_3 as base, DMF as a solvent, under inert conditions and RT were chosen as standard conditions. Iodobenzene and methyl acrylate were used as the halide and alkene respectively. Iodobenzene has a weaker bond than C-Br and C-Cl bonds in which will be beneficial. Moreover, methyl acrylate is an activated alkene which will be advantageous in increasing the reactivity.

Table 3-3 Heck C-C cross-coupling reaction between Iodobenzene and methyl acrylate

Entry	Catalyst system	Deviation from conditions	^{1}HNMR Yield (%)
1	$(4\text{-Py-BDP})_2PdCl_2$	No base	0
2	-	No catalyst	0
3	$(4\text{-Py-BDP})_2PdCl_2$	No light	0
4	Pd $(Py)_2Cl_2$	None	10%
5	Pd $(Py)_2Cl_2$ + BODIPY	None	13%
6	$(4\text{-Py-BDP})_2PdCl_2$	None	29%
7	$(3\text{-Py-BDP})_2PdCl_2$	None	46%
8	$(2\text{-Py-BDP})_2PdCl_2$	None	28%

As shown in Table 3-3, several reaction conditions were tested. Entries 1-3, different reaction conditions were used. In entry 1 no base used, in entry 2 no catalyst used, entry 3 no light used. In entries 4-8 all the condition that mentioned were used with different catalysts system. Among all the entries, entry 7 produced the highest yield. Entry 6 and 8 came after that. Entries 4 indicates the importance of the involvement of BODIPY in the reaction when compared to 5-8 entries. Whereas entry 6 indicates that lower yield will be obtained when a BODIPY and Pd catalyst was used instead of BODIPY is being chemically bonded to the catalyst. Entries 1-3 demonstrated that K_2CO_3, Pd catalyst, and light are crucial to the reaction.

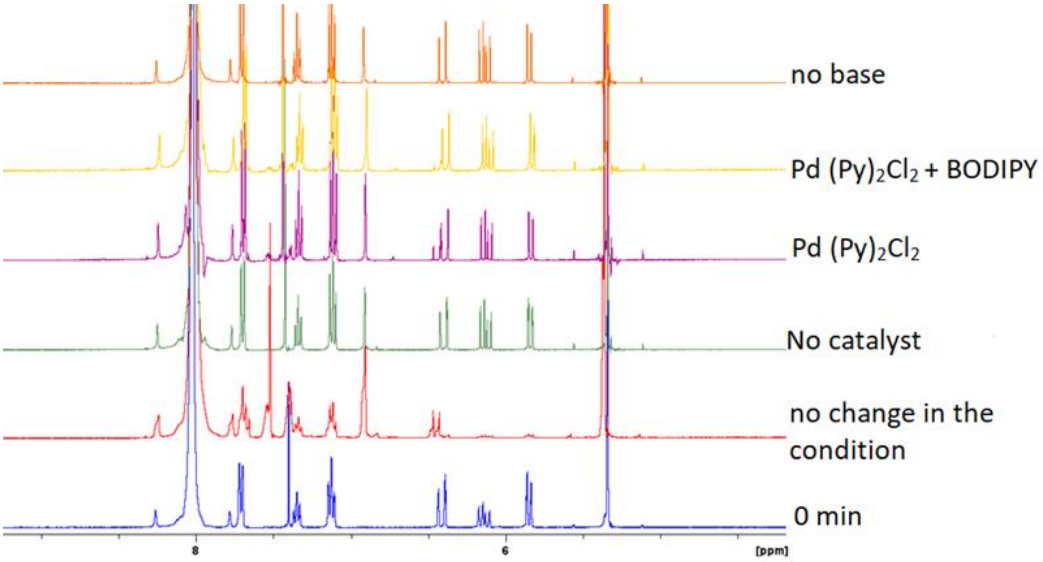

Figure 3-12 ^{1}HNMR spectra of a reaction mixture of Iodobenzene and methyl acrylate under different conditions. The spectra was collected in DMF

3.5.2 Substituent effect on Heck C-C cross-coupling reaction between methyl acrylate and iodobenzene

A variety of iodobenzene derivatives were used to examined the substituent effect of the photocatalyzed Heck C-C cross-couplings reactions for three different Py-BODIPY-Pd catalysts.

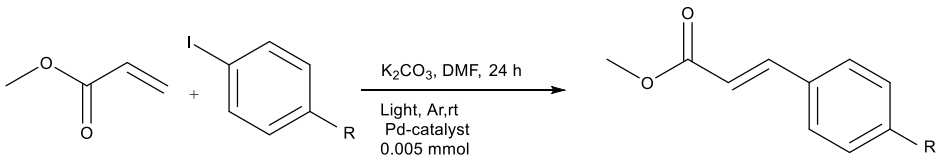

Table 3-4 Heck C-C cross-coupling reactions with substituted iodobenzene when 4-Py-BODIPY-Pd catalyst was used

Entry	R	^{1}H NMR Yield (%)
1	Cl	18%
2	NH_2	80%
3	COOMe	62%
4	CH_3	28%
5	CN	11%
6	CHO	61%
7	OCH_3	74%
8	COOEt	37%
9	NO_2	10%
10	Tert-Butyl	30%
11	Pyridine	55%

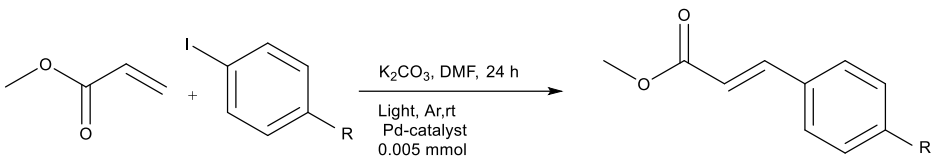

Table 3-5 Heck C-C cross-coupling reactions with substituted iodobenzene when 3-Py-BODIPY-Pd catalyst was used

Entry	R	^{1}HNMR Yield (%)
1	Cl	23%
2	NH_2	54%
3	CH_3	53%
4	CN	12%
5	CHO	43%
6	OCH_3	27%

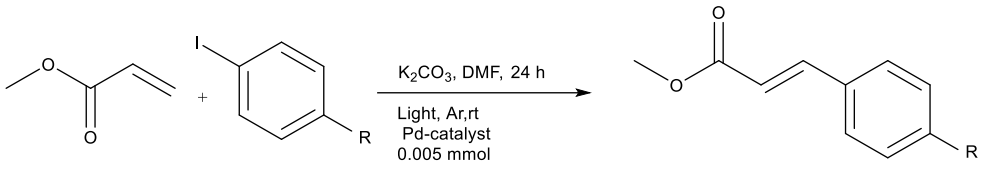

Table 3-6 Heck C-C cross-coupling reactions with substituted iodobenzene when 2-Py-BODIPY-Pd catalyst was used

Entry	R	^{1}HNMR Yield (%)
1	Cl	20%
2	NH_2	67%
3	COOMe	38%
4	CH_3	41%
5	CN	21%
6	CHO	82%
7	OCH_3	45%

When various substituted aryl iodides were examined, it can be observed that the yields of the desired products were generally higher than that of the model reaction when electron donating groups derivatives were used whereas lower yields were obtained when electron withdrawing groups were used. This observation can be associated with the influence of electron donating or electron withdrawing substitutions. As seen in the tables above ED substitutions activate the benzene ring toward electrophilic attack, on the other hand EW substitutions deactivate the benzene ring toward electrophilic attack. ED substitutions can donate their electrons in the system and stabilize the positive charge that build up in the rate limiting step which

decreased the energy of the intermediate and increased the energy of the starting material. In contract, EW substations destabilize the positive charge by raising the energy of the transition state.

It is obvious here that the substituents in the para position has a significant interaction with the development of the positive charge which indicate that these reactions will have a steep slope for their Hammett plots. Electron donating groups such as a methoxy will speed up the reaction rate constant because they can flow electron density into the developing positive charge and that will stabilize it. On the other hand, electron withdrawing groups such as trifluoromethyl is going to pull electron density away from the developing positive charge which will very destabilizing which will slow down the reaction. From this observation, we can estimate that Rho value will be significant which is also an indication that the reaction is an SN_1 reaction mechanism.

4 Conclusions and future work

Heck C-C cross-coupling reaction is fundamentally important reaction that have attracted a lot of attention in synthetic organic chemistry because of their high efficiency and simplicity. The coupling of halides and terminal alkenes by phosphine-ligated palladium complexes is regarded as the most important and widely used method of preparing a substituted alkene with high reactivities and selectivities. However, this method includes undesired condition such as high temperature, higher loading of catalyst, and high toxicity. To overcome the disadvantages of the conventional method, several studies have been done over the past years. These studies include heterogenous catalysis, and reactions in aqueous media. Heterogenous catalysts are recognized to have lower activity than homogeneous catalysts.[54] In this research a highly efficient homogeneous photocatalyst based on BODIPY for the Heck C-C cross-coupling reactions of aryl iodide and methyl acrylate

in DMF solvent under inert conditions has been developed. The 4-Py-BDP-Pd, 3-Py-BDP-Pd and, 2-Py-BOD-Pd catalysts were synthesized and purified using column chromatography. The optical properties of products and the intermediates were investigated by UV/vis absorption and fluorescence spectroscopy. Catalysts were used for the Heck C-C cross-coupling reaction between iodobenzene and methyl acrylate and successfully produced a substituted alkene with high reactivities under mild condition. Heck C-C cross-coupling reactions of a wide range of iodobenzene with methyl acrylate have been done to evaluate the substrate scope of the photocatalyzed Heck C-C cross-coupling reactions. when electron donating groups derivatives were used, desired products yields were higher than that of the model reaction. Meanwhile, lower yields were obtained when electron withdrawing groups were used.

Future work would include the usage of different nucleophilic and electrophilic starting materials. Bromobenzene electrophilic could be used instead of iodobenzene in which is cheaper than iodobenzene and wide range of alkene can be tested. Several mechanistic studies can be conducted such as cyclic voltammetry and other different studies, in order to gain some information about the mechanism.

References

1. Augustine, R. L., CRC Press.**1979,** Vol. 1.

2. Kloetzel, M. C. Top. Catal. **2002,** 19, 101–109.

3. Tamao, K.; Sumitani, K.; Kumada, M., J. Am. Chem. Soc. **1972,** 94 (12), 4374-4376.

4. Maercker, A. Org. React. **1965,** 14, 270–490.

5. Little, R. D.; Masjedizadeh, M. R.; Wallquist, O.; McLoughlin, J. I. Org. React. **1995,** 47, 315–552.

6. Veerakumar, P.; Thanasekaran, P.; Lu, K.-L.; Lin, K.-C.; Rajagopal, S., ACS Sustainable Chem. Eng. **2017,** 5(10), 8475-8490.

7. Bolm, C.; Beller, M. Wiley-VCH: Weinheim. **2004,** Vol. 1.

8. Veerakumar, P.; Thanasekaran, P.; Lu, K.-L.; Lin, K.-C.; Rajagopal, S., ACS Sustainable Chem. Eng. **2017,** 5 (10) , 8475-8490.

9. Johansson Seechurn, C. C. C.; Kitching, M. O.; Colacot, T. J.; Snieckus, V. Angew. Chem., Int. Ed. **2012,** 51, 5062−5085.

10. Beletskaya, I.; Cheprakov, A. V. Chem. Rev. **2000,** 100 (8), 3009–3066.

11. Mizoroki, T.; Mori, K.; Ozaki, A. Bull. Chem. Soc. Jpn. **1971,** 44, 581.

12. Heck, R. F.; Nolley, J. P. J. Org. Chem. **1972,** 37, 2320–2322.

13. Crisp, G. T. Chem. Soc. Rev. **1998,** 27, 427–436.

14. Link, J. T.; Overman, L. E. Diedrich, F.; Stang, P. J., Eds.; Wiley-VCH: Weinheim, Germany. **1998.**

15. Beletskaya, I.; Cheprakov, A. V. Chem. Rev. **2000,** 100, 3009–3066.

16. Liu, L.-j.; Wang, F.; Wang, W.; Zhao, M.-x.; Shi, M. Beilstein J. Org. Chem. **2011,** 7, 555–564.17. Grasa, G. A.; Singh, R.; Stevens, E. D.; Nolan, S. P. J. Organomet. Chem. **2003,** 687, 269–279.

18. Ozawa, F.; Kubo, A.; Hayashi, T. Chem. Lett. **1992,** 2177–2180.

19. Littke, A. F.; Fu, G. C. J. Org. Chem. **1999**, 64, 10–11.

20. Stambuli, J. P.; Stauffer, S. R.; Shaughnessy, K. H.; Hartwig, J. F. J. Am. Chem. Soc. **2001,** 123, 2677–2678.

21. Hansen, A. L.; Ebran, J.-P.; Ahlquist, M.; Norrby, P.-O.; Skrydstrup, T. Angew. Chem., Int. Ed. **2006,** 45, 3349–3353.

22. Fleckenstein, C. A.; Plenio, H. Chem. Soc. Rev. **2010,** 39, 694–711.

23. Blaser, H.U.; Indolese, A.; Schnyder, A. Curr. Sci. **2000,** 78, 1336–1344.

24. De Vries, J.G. Can. J. Chem. **2001,** 79, 1086–1092.

25. Cabri, W.; Candiani, J. Am. Chem. Soc. **1995,** 28 (1), 2-7.

26. G. T. Crisp, Chem. Soc. Rev. **1998,** 27, 427.

27. Yoon, T. P.; Ischay, M. A.; Du, J., Nature Chem. **2010,** 2 (7), 527.

28. P. T. Anastas, J. C. Warner, Green Chemistry. **1998.**

29. D. Cambie, C. Bottecchia, N. J. W. Straathof, V. Hessel, T. Noel, Chem. Rev. **2016,** 116, 10276–10341.

30. Romero, N.A. & Nicewicz, D.A. *Chemical Reviews*. **2016,** 116, 10075-100116.

31. Akita, M. & Koike, T. J. Syn. Org. Chem. Jpn. **2016**, 1036-1046.

32. K. Ohkubo, A. Fujimoto and S. Fukuzumi , J. Am. Chem. Soc., **2013,** 135 (14), 5368 —5371.

33. Narayanam, J. M.R.; Stephenson, C.R.J., The Royal Society of Chemistry **2011,** 40, 102-113.

34. Prier, C. K.; Rankic, D. A.; MacMillan, D. W., Chem. Soc. Rev. **2013,** 113 (7), 5322-5363.

35. Zhou, Q.; Zou, Y.; Lu, L.; Xiao, W., Angew Chem Int Ed Engl. **2019,** 58(6),1586-1604.

36. Skubi, K.; Blum, T.; Yoon, T., Chem. Soc. Rev. 2016, 116 (17), 10035- 10074.

37. Treibs, A.; Kreuzer, F.-H. Liebigs Ann. Chem. **1968,** 718, 208− 223.

38. Boens, N.; Leen, V.; Dehaen, W. Chem. Soc. Rev. **2012,** 41, 1130− 1172.

39. Valeur, B., Wiley-VCH: Weinheim, Germany, **2002.**

40. Boens, N. I.; Leen, V.; Dehaen, W.; Wang, L.; Robeyns, K.; Qin, W.; Tang, X.; Beljonne, D.; Tonnele, C.; Paredes, J. M., J Phys. Chem. A 2012, 116 (39), 9621-9631.

41. J. W. Tucker and C. R. J. Stephenson, *J.* Org. *Chem.*, **2012,** 77, 1617.

42. Huang, L.; Zhao, J., Chem. Commun. **2013,** 49 (36), 3751-3753.

43. Guo, S.; Tao, R.; Zhao, J., SC Adv., **2014**,4, 36131-36139.

42.Cui, A.; Peng, X.; Fan, J.; Chen, X.; Wu, Y.; Guo, B.; Journal of Photochemistry and Photobiology A: Chemistry. **2007,** 186, 85-92.

43. Shrestha, M.; Si, L.; Chang, C; He, H.; Sykes, A.; Lin, C.; Diau, E., J. Phys. Chem. **2012,** 116 (19), 10451−10460.

44. Dissanayake, K.; Ebukuyo, P.; Dhahir, Y.; Wheeler, K.; He, H., Chem. Commun. **2019**, 55, 4973-4976.

45. Qin, W.; Baruah, M.; Borggraeve, W.; Boens, N., Journal of Photochemistry and Photobiology A: Chemistry. **2006,** 183, 190–197.

46. Cabanillas-Galán, P.; Farmer, L.; Hagan, T.; Nieuwenhuyzen, M.; James, S. L.; Lagunas, M. C., A. Inorg. Chem. **2008,** 47, 9035-9041.

47. Jiang, J.; Zhang, W.; Dai, J.; Xu, J.; Xu, H., The J. Org. Chem. **2017,** 82.

48. Mahajan, S.; Singh, IP., Magn Reson Chem. **2013,** 51, 76-81.

49. Andreu, A. Zapf, M. Beller, Chem. Commun.**2000,** 2475–2476.

50. Huang, L.; Zhao, J.; Guo, S.; Zhang, C.; Ma, J., J Org. Chem. **2013,** 78 (11), 5627-5637.

51. Zhao, J.; 92 Xu, K.; Yang, W.; Wang, Z.; Zhong, F., Chem. Soc. Rev. **2015,** 44 (24), 8904-8939.

52. Bakherad, M.; Keivanloo, A.; Bahramian, B.; Karnali, T. A., J Braz. Chem. Soc. **2009,** 20 (5), 907-

A. APPENDICES

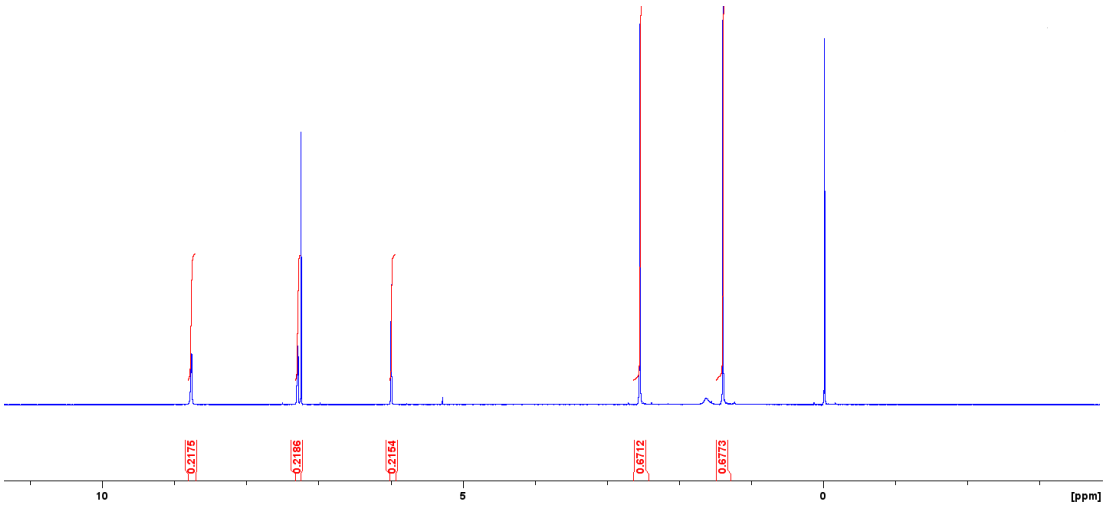

Figure A-1 ^{1}H NMR spectrum of 4-Py-BDP. The spectrum was collected in $CDCl_3$

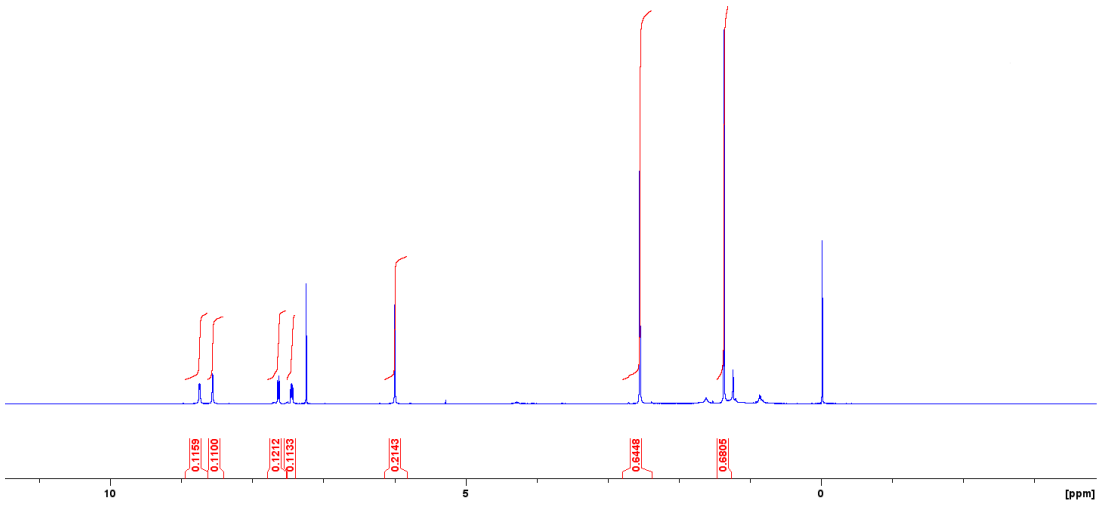

Figure A-2 ^{1}H NMR spectrum of 3-Py-BDP. The spectrum was collected in $CDCl_3$

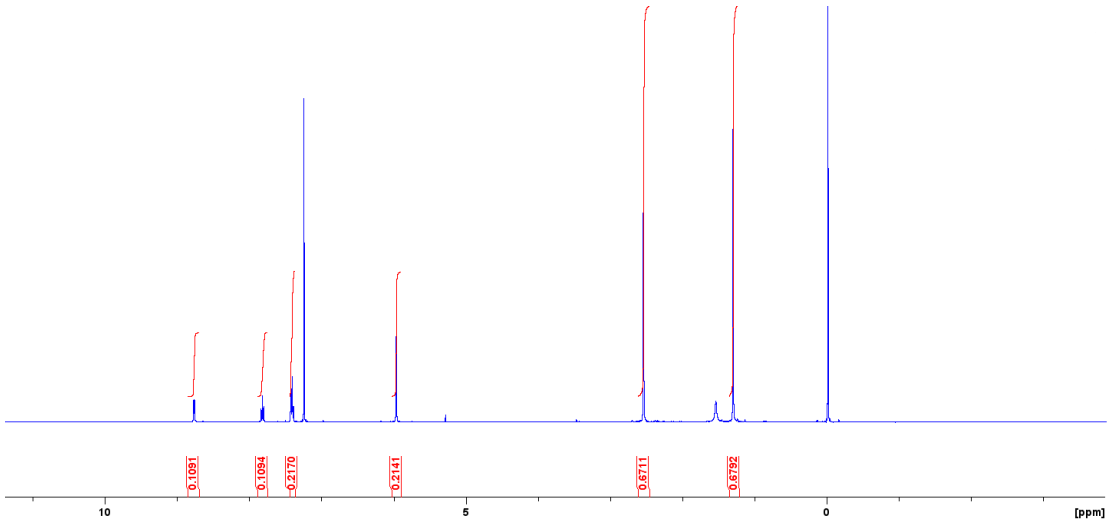

Figure A-3 ^{1}H NMR spectrum of 2-Py-BDP. The spectrum was collected in $CDCl_3$

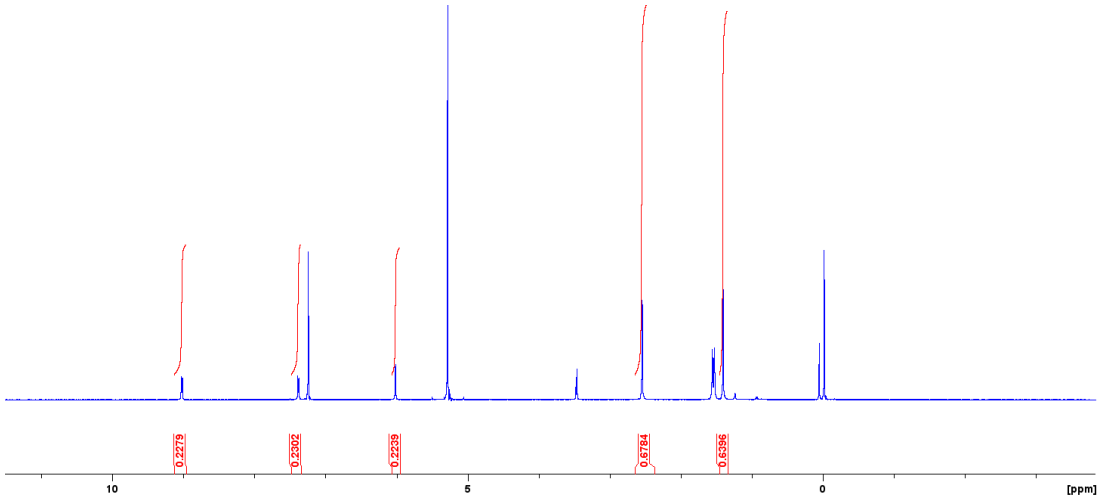

Figure A-4 ^{1}H NMR spectrum of 4-Py-BDP-Pd. The spectrum was collected in $CDCl_3$

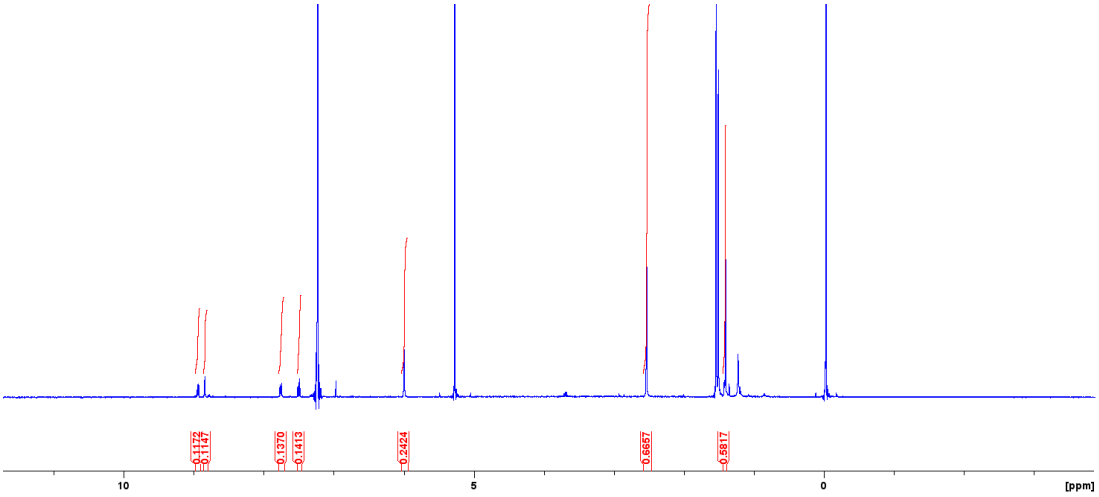

Figure A-5 ^{1}H NMR spectrum of 3-Py-BDP-Pd. The spectrum was collected in $CDCl_3$

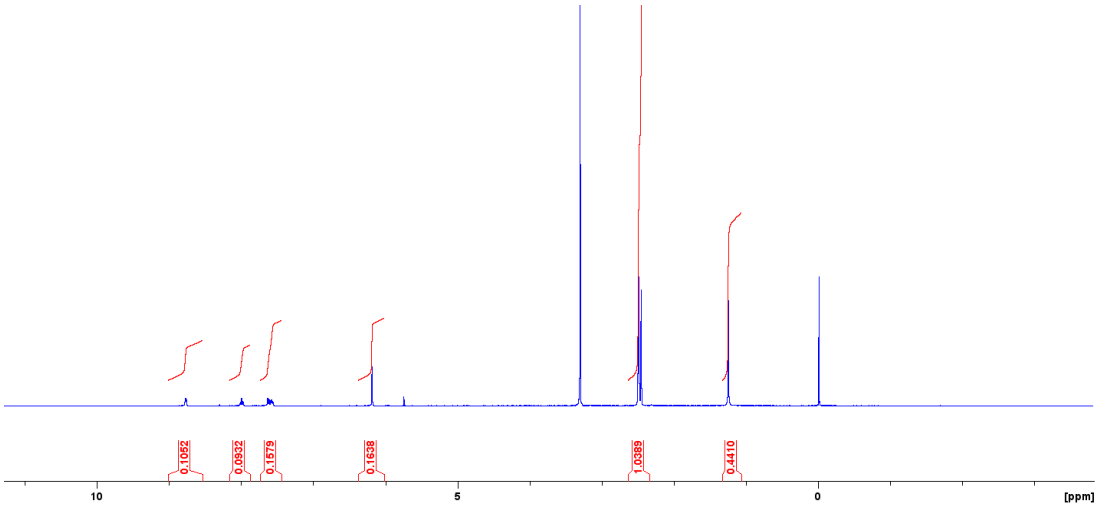

Figure A-6 ^{1}H NMR spectrum of 2-Py-BDP-Pd. The spectrum was collected in DMSO

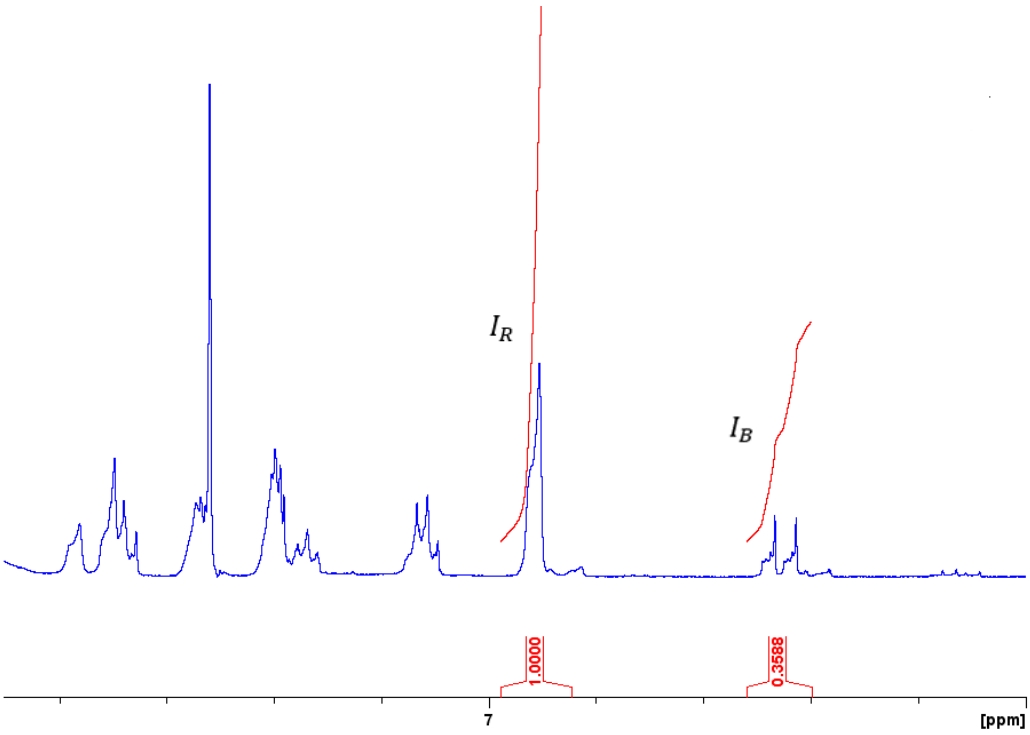

Figure A-7 ^{1}H NMR spectrum of a reaction mixture of iodobenzene and methyl acrylate using 4-Py-BDP-Pd as a catalyst. The spectrum was collected in $CDCl_3$

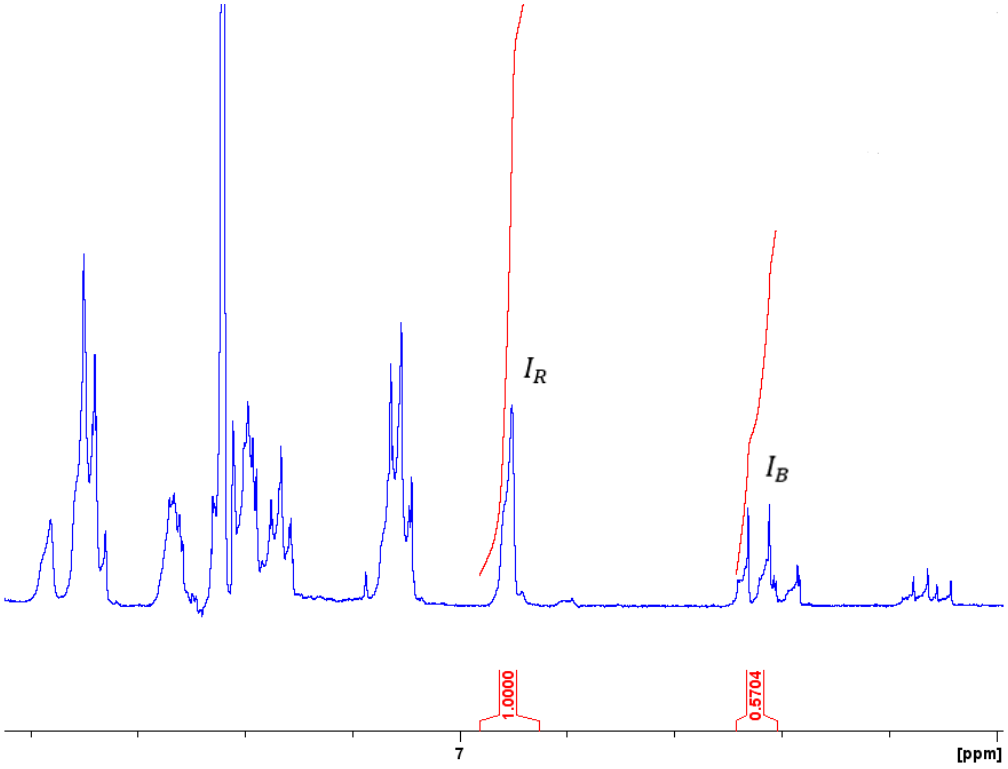

Figure A-8 ^{1}H NMR spectrum of a reaction mixture of iodobenzene and methyl acrylate using 3-Py-BDP-Pd as a catalyst. The spectrum was collected in $CDCl_3$

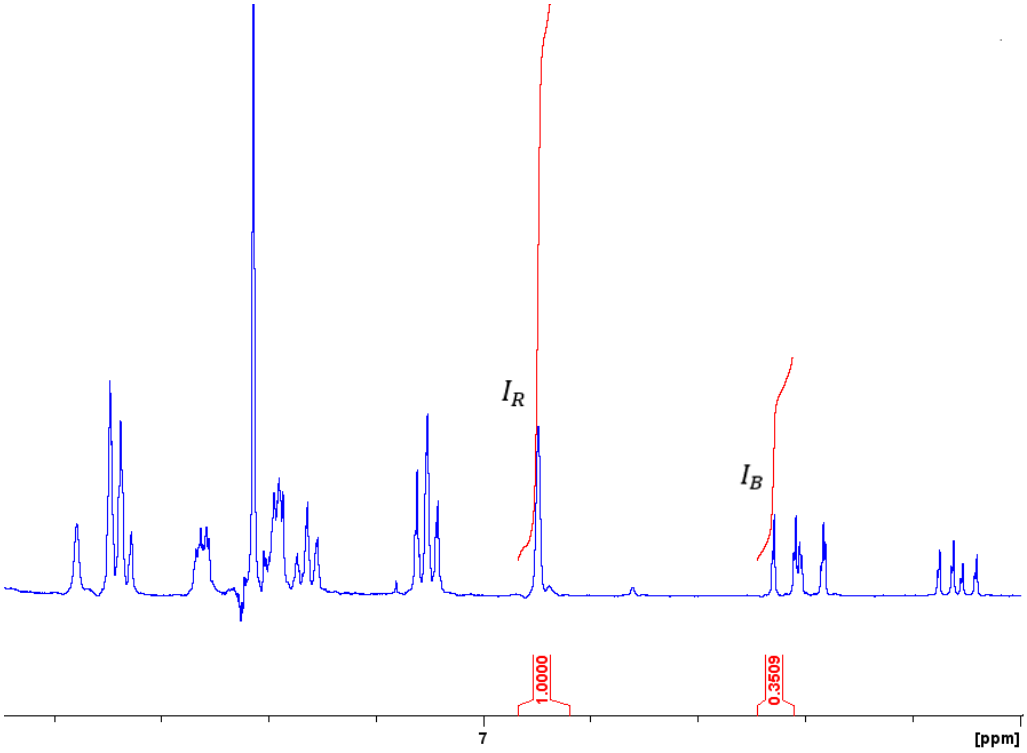

Figure A-9 ^{1}H NMR spectrum of a reaction mixture of iodobenzene and methyl acrylate using 2-Py-BDP-Pd as a catalyst. The spectrum was collected in $CDCl_3$

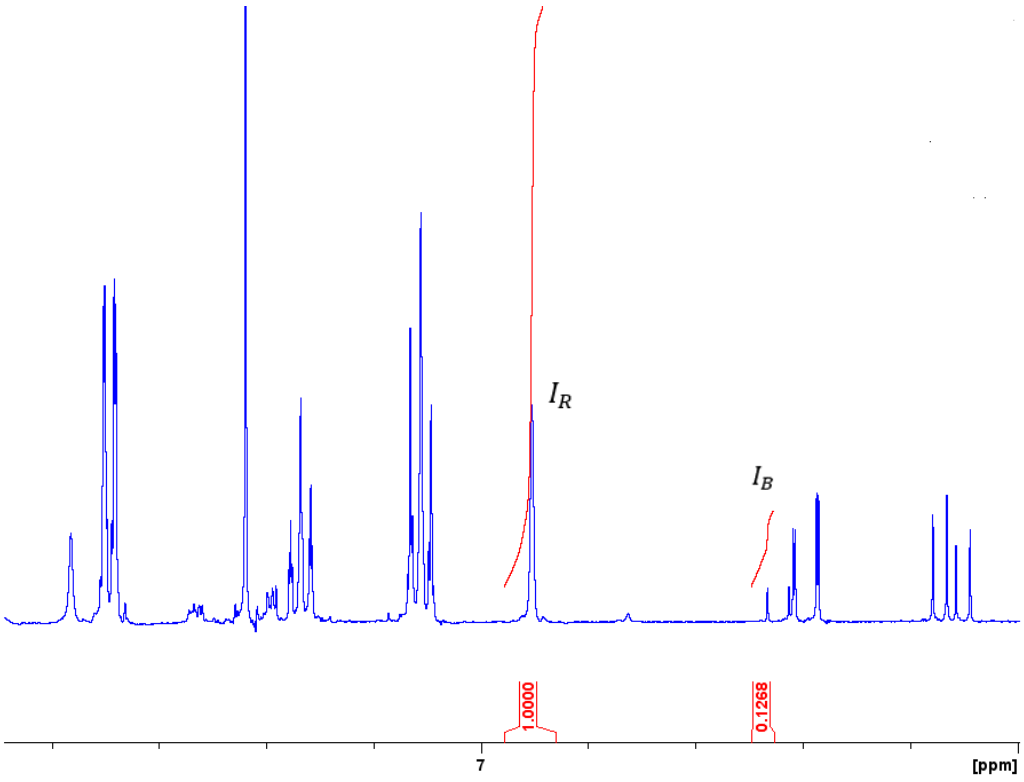

Figure A-10 ^{1}H NMR spectrum of a reaction mixture of iodobenzene and methyl acrylate using 2-Py-BDP-Pd as a catalyst. The spectrum was collected in $CDCl_3$

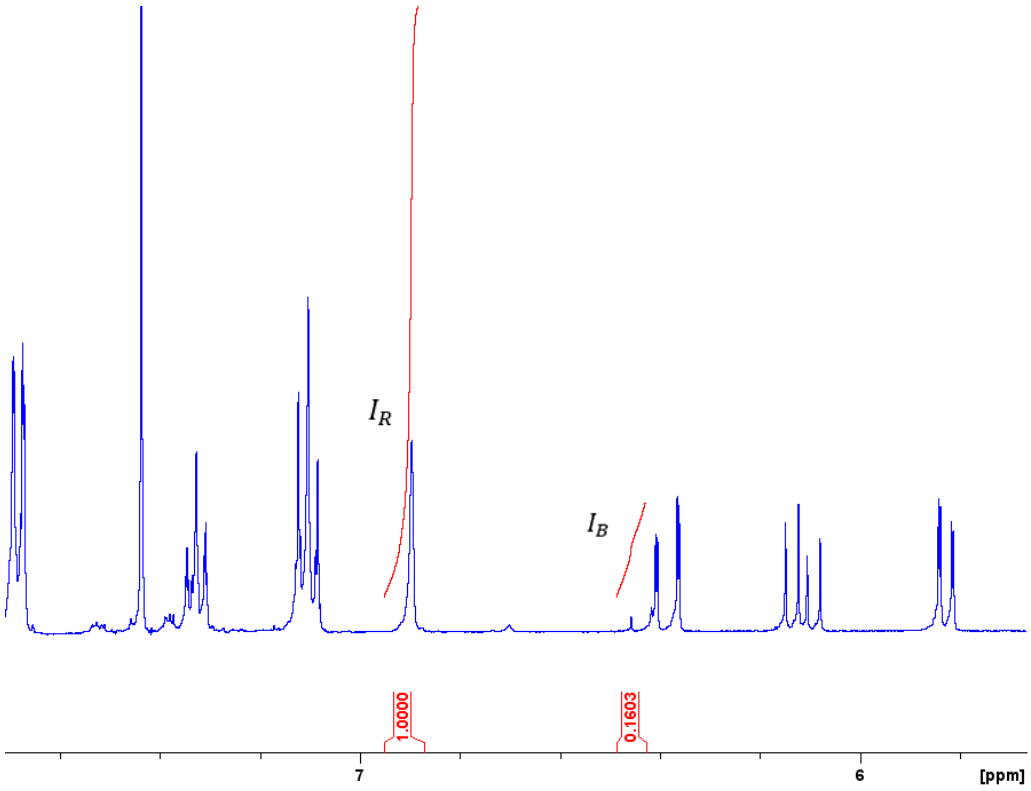

Figure A-11 ^{1}H NMR spectrum of a reaction mixture of iodobenzene and methyl acrylate using 2-Py-BDP-Pd as a catalyst. The spectrum was collected in $CDCl_3$

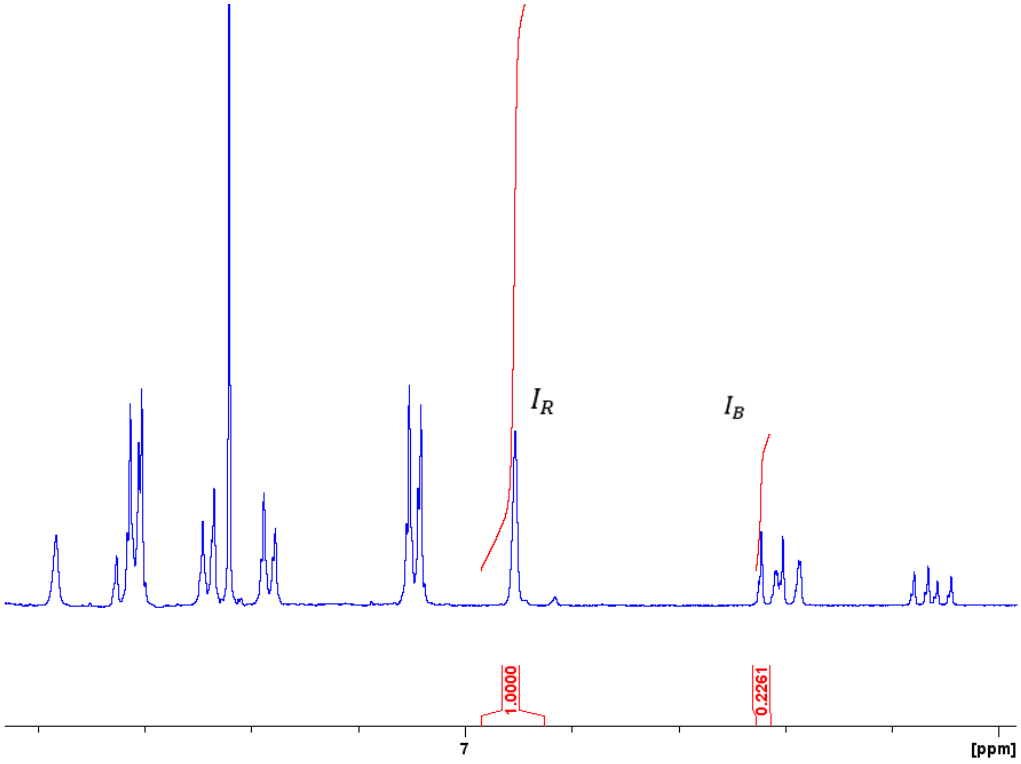

Figure A-12 ^{1}H NMR spectrum of a reaction mixture of 1-chloro-4- iodobenzene and methyl acrylate using 4-Py-BDP-Pd as a catalyst. The spectrum was collected in $CDCl_3$

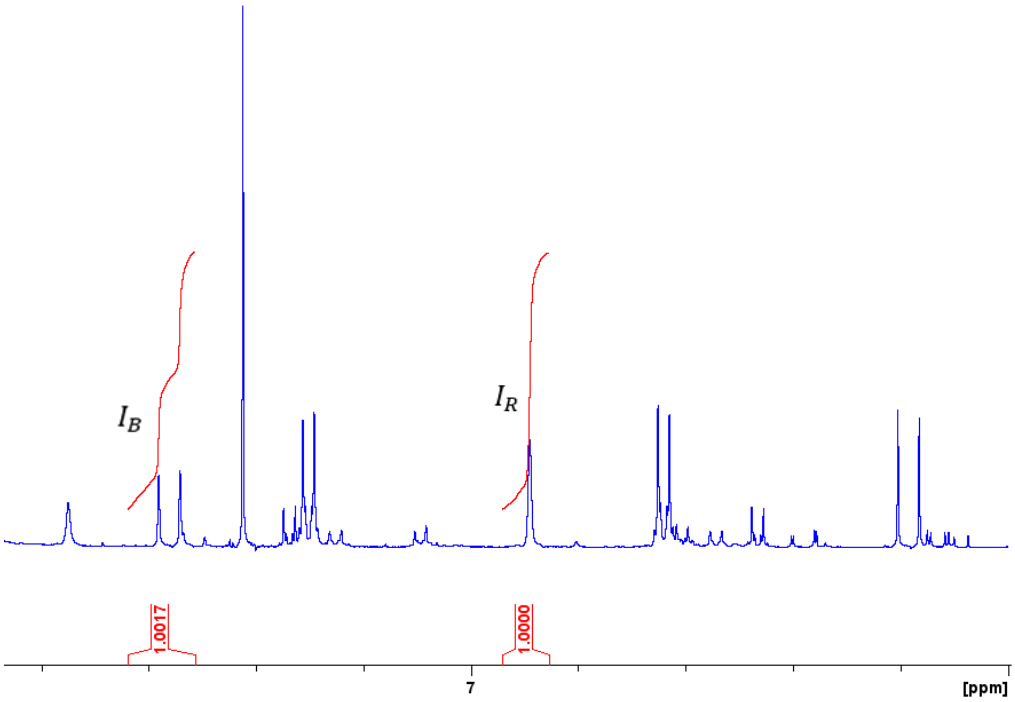

Figure A-13 ^{1}H NMR spectrum of a reaction mixture of 1-chloro-4- iodobenzene and methyl acrylate using 4-Py-BDP-Pd as a catalyst. The spectrum was collected in $CDCl_3$

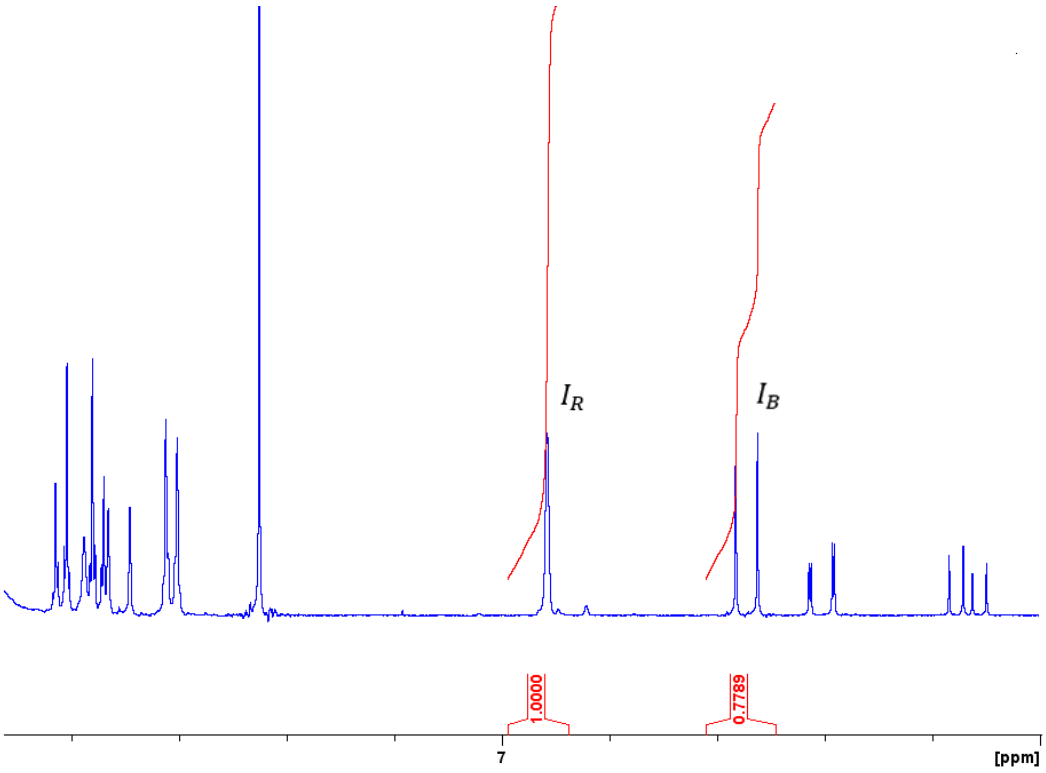

Figure A-14 ^{1}H NMR spectrum of a reaction mixture of 4-methyl-4-iodobenzoate and methyl acrylate using 4-Py-BDP-Pd as a catalyst. The spectrum was collected in $CDCl_3$

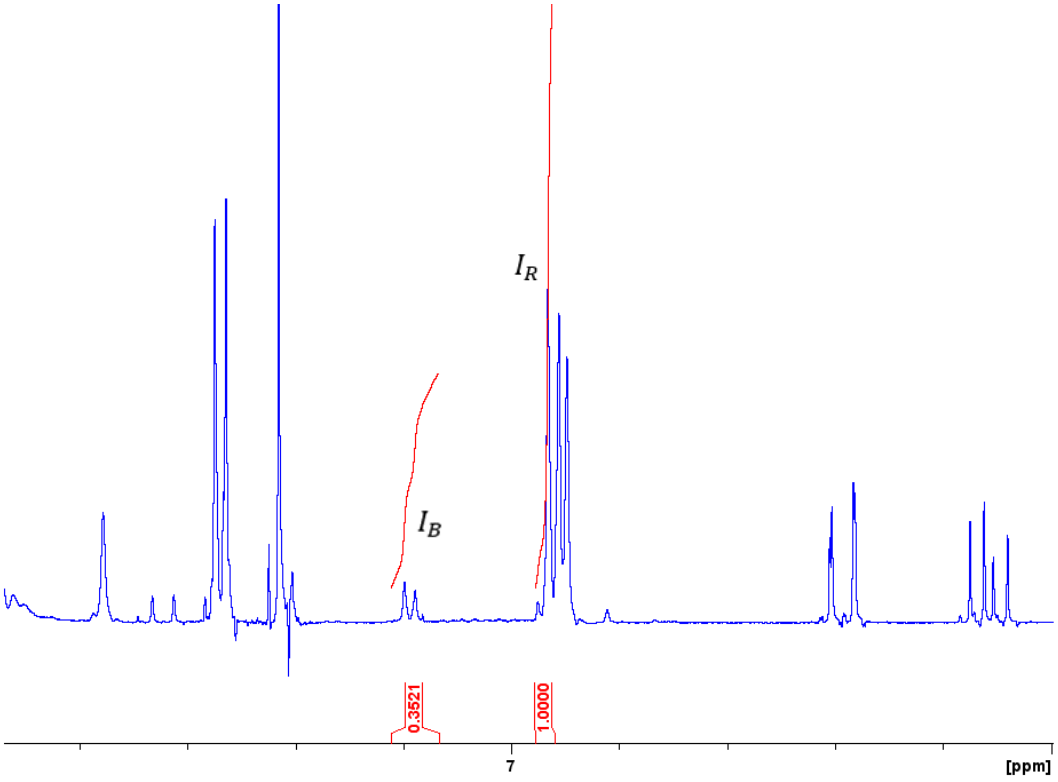

Figure A-15 ^{1}H NMR spectrum of a reaction mixture of 4-iodotoluene and methyl acrylate using 4-Py-BDP-Pd as a catalyst. The spectrum was collected in $CDCl_3$

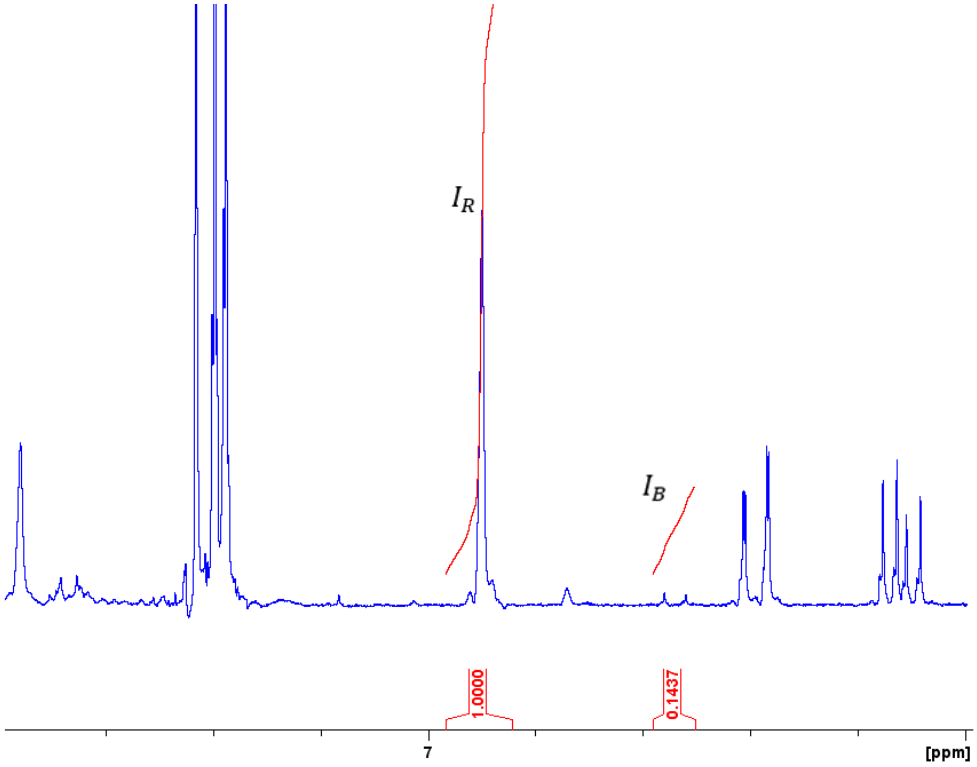

Figure A-16 ^{1}H NMR spectrum of a reaction mixture of 4-iodobenzonitrile and methyl acrylate using 4-Py-BDP-Pd as a catalyst. The spectrum was collected in $CDCl_3$

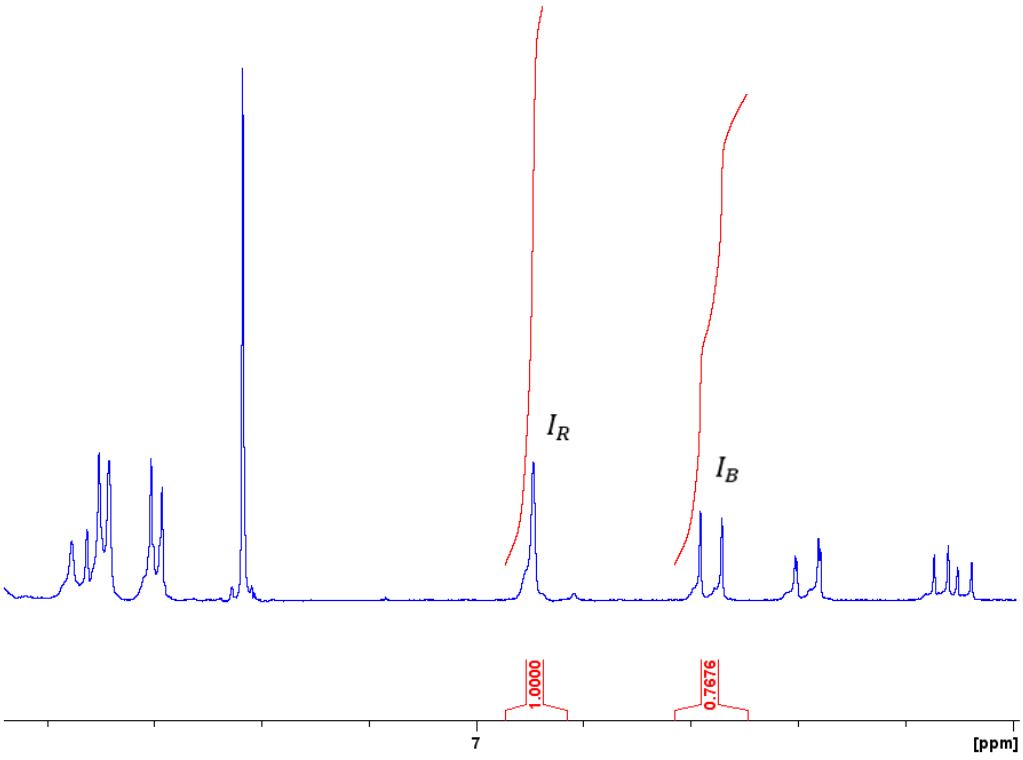

Figure A-17 ^{1}H NMR spectrum of a reaction mixture of 4-iodobenzaldhyde and methyl acrylate using 4-Py-BDP-Pd as a catalyst. The spectrum was collected in $CDCl_3$

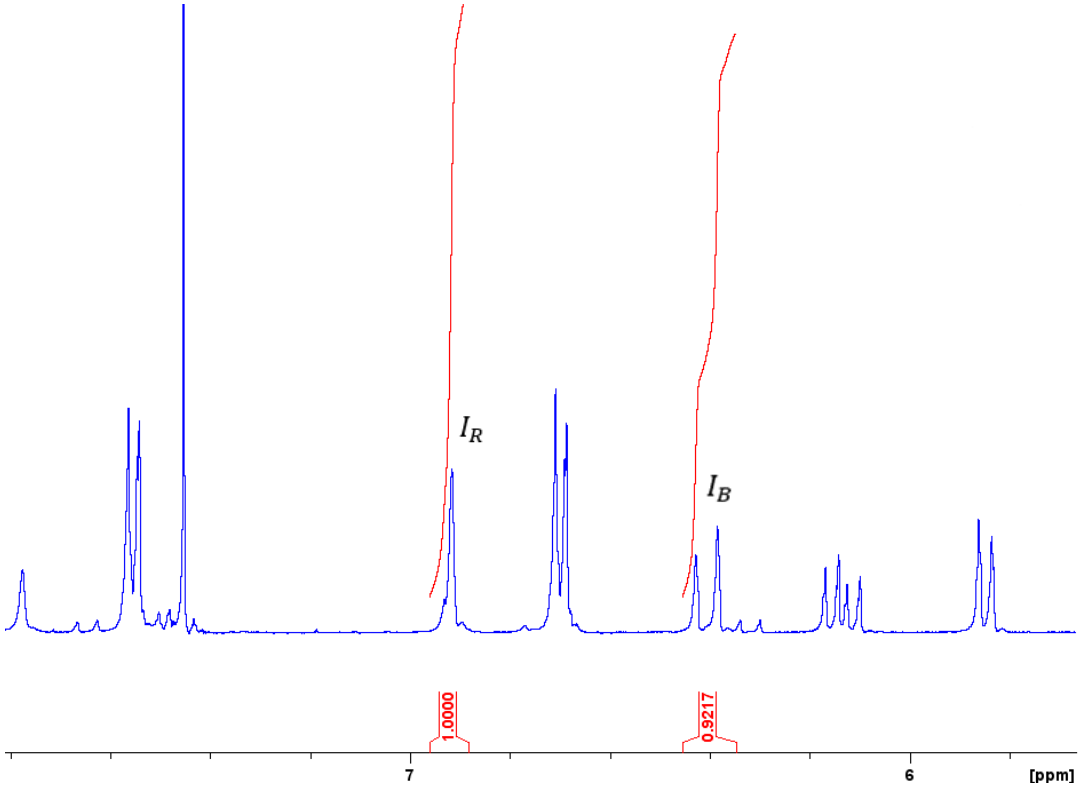

Figure A-18 ^{1}H NMR spectrum of a reaction mixture of 1-iodo-4-methoxybenzene and methyl acrylate using 4-Py-BDP-Pd as a catalyst. The spectrum was collected in $CDCl_3$

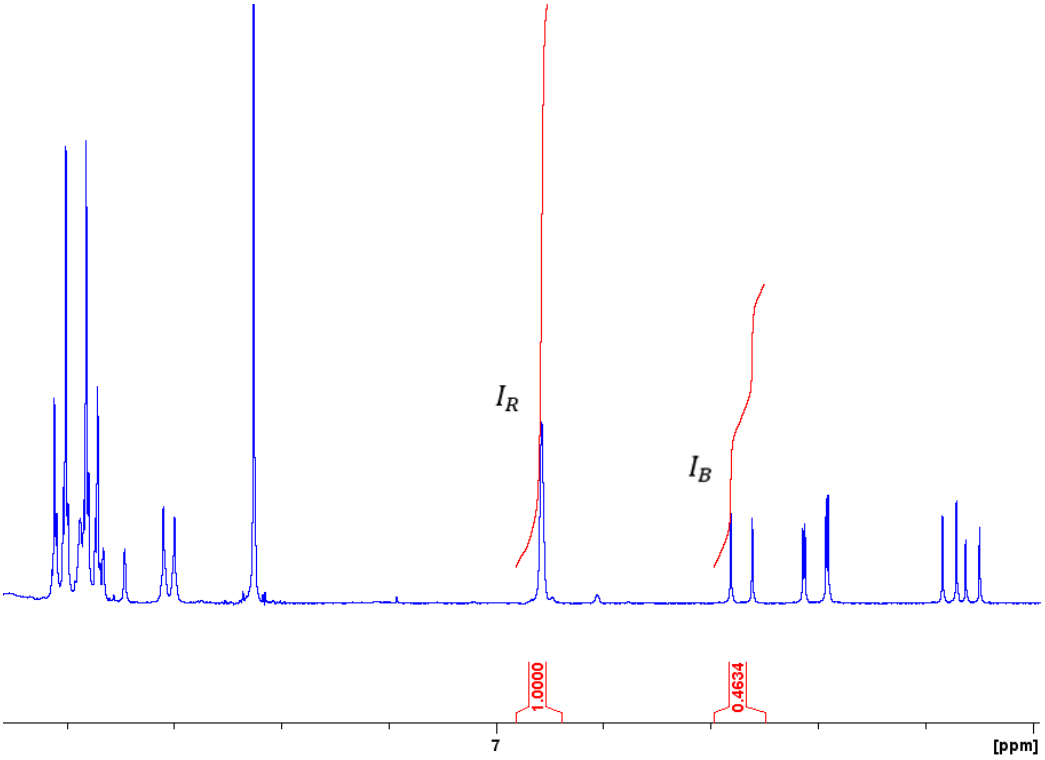

Figure A-19 ^{1}H NMR spectrum of a reaction mixture of ethyl-4-iodobenzoate and methyl acrylate using 4-Py-BDP-Pd as a catalyst. The spectrum was collected in $CDCl_3$

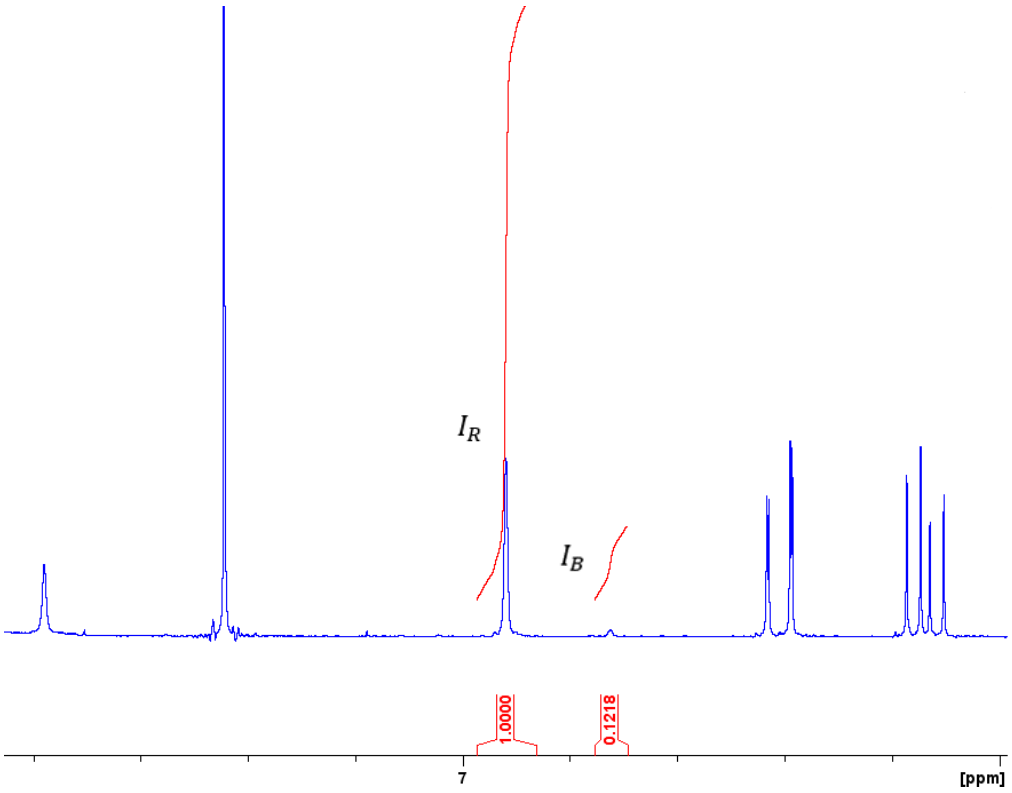

Figure A-20 ^{1}H NMR spectrum of a reaction mixture of 1-iodo-4-nitrobenzene and methyl acrylate using 4-Py-BDP-Pd as a catalyst. The spectrum was collected in $CDCl_3$

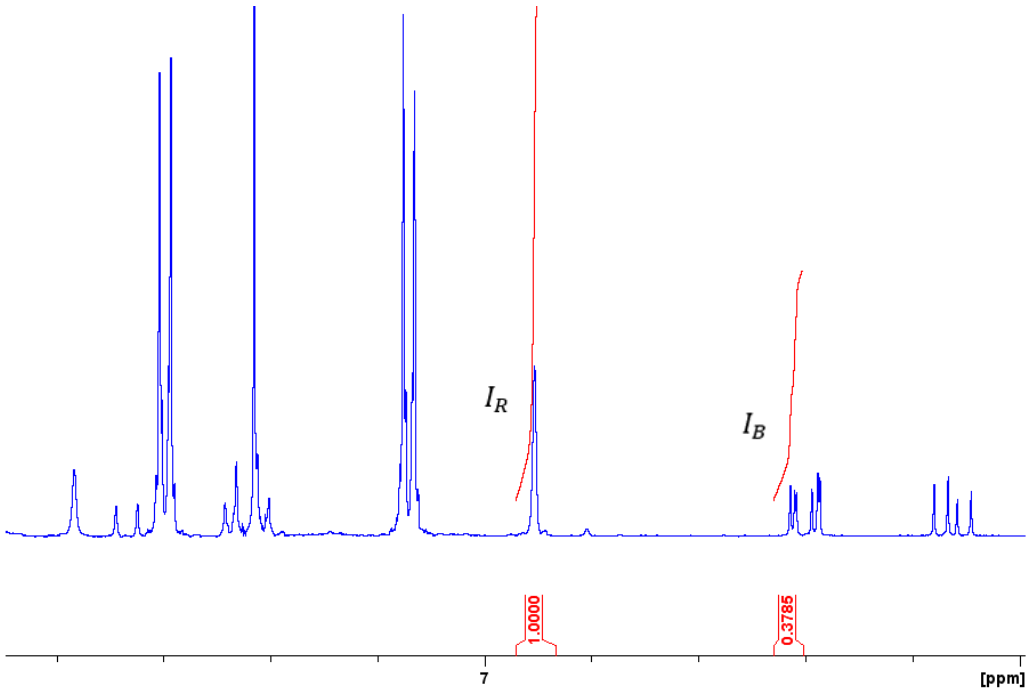

Figure A-21 ^{1}H NMR spectrum of a reaction mixture of 1-tert-Butyl-4-iodobenzene and methyl acrylate using 4-Py-BDP-Pd as a catalyst. The spectrum was collected in $CDCl_3$

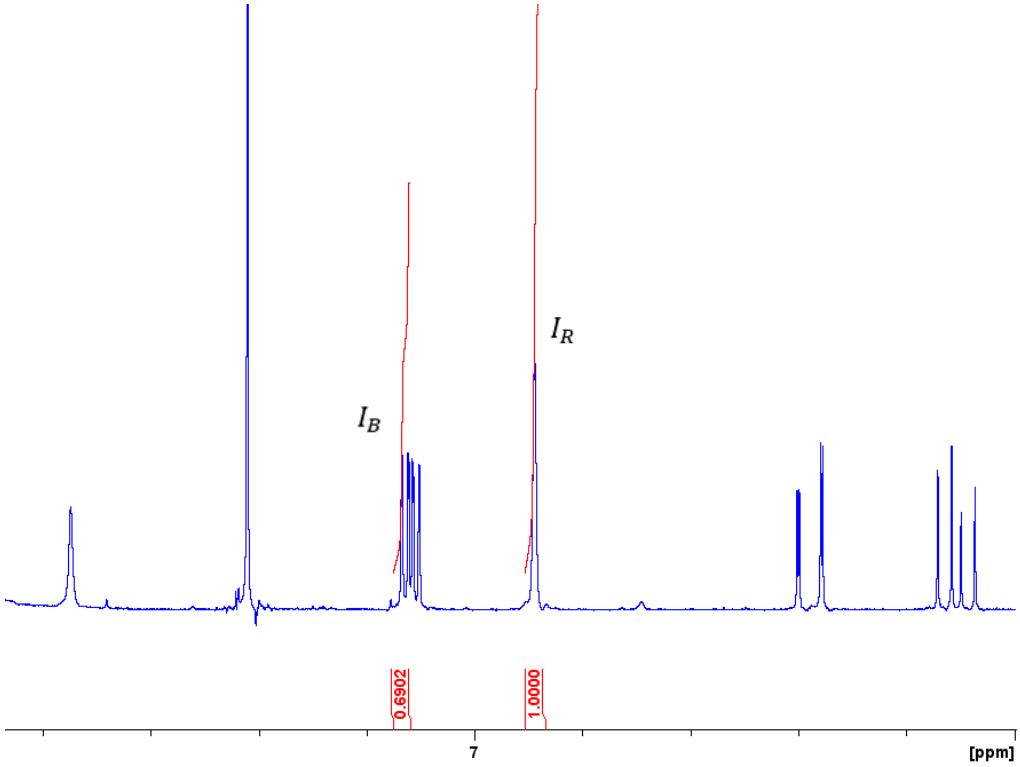

Figure A-22 ^{1}H NMR spectrum of a reaction mixture of 3-iodopyridine and methyl acrylate using 4-Py-BDP-Pd as a catalyst. The spectrum was collected in $CDCl_3$

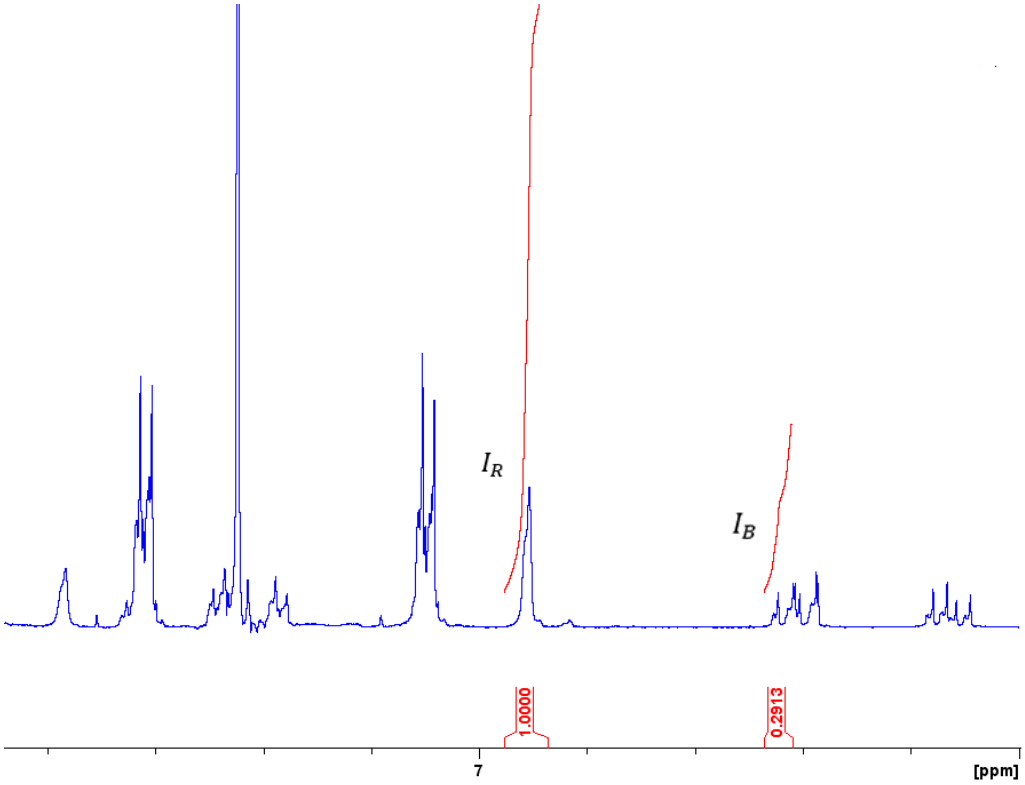

Figure A-23 ^{1}H NMR spectrum of a reaction mixture of 1-chloro-4-iodobenzene and methyl acrylate using 3-Py-BDP-Pd as a catalyst. The spectrum was collected in $CDCl_3$

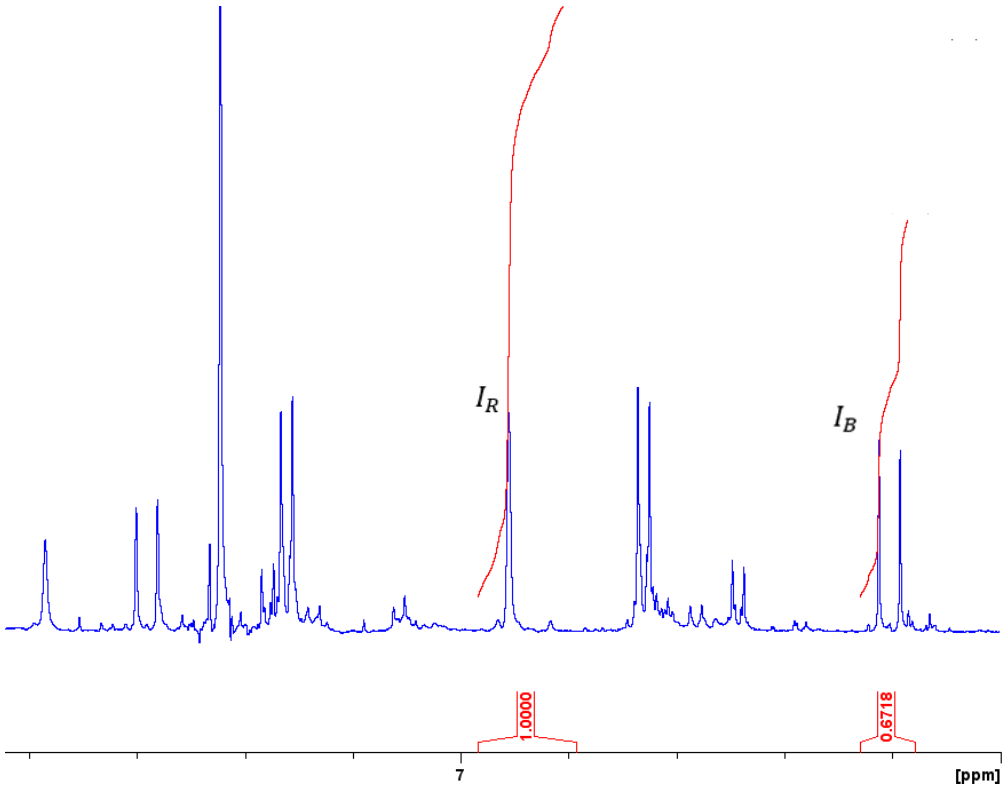

Figure A-24 ^{1}H NMR spectrum of a reaction mixture of 4-iodoaniline and methyl acrylate using 3-Py-BDP-Pd as a catalyst. The spectrum was collected in $CDCl_3$

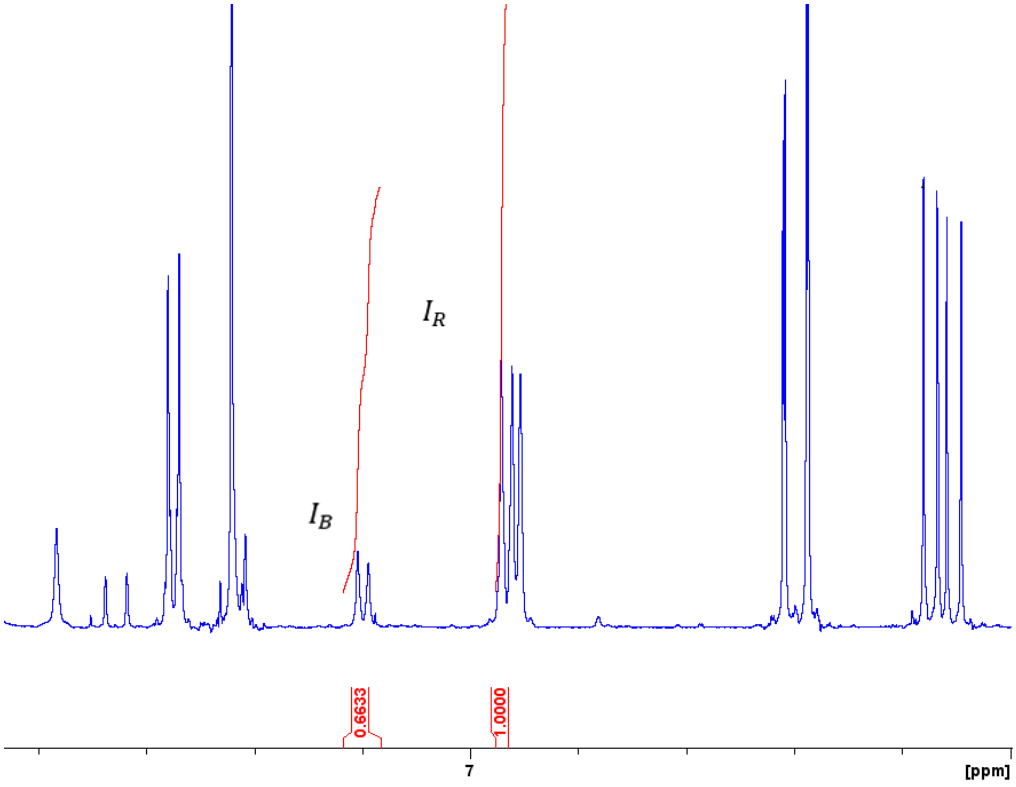

Figure A-25 ^{1}H NMR spectrum of a reaction mixture of 4-iodotoluene and methyl acrylate using 3-Py-BDP-Pd as a catalyst. The spectrum was collected in $CDCl_3$

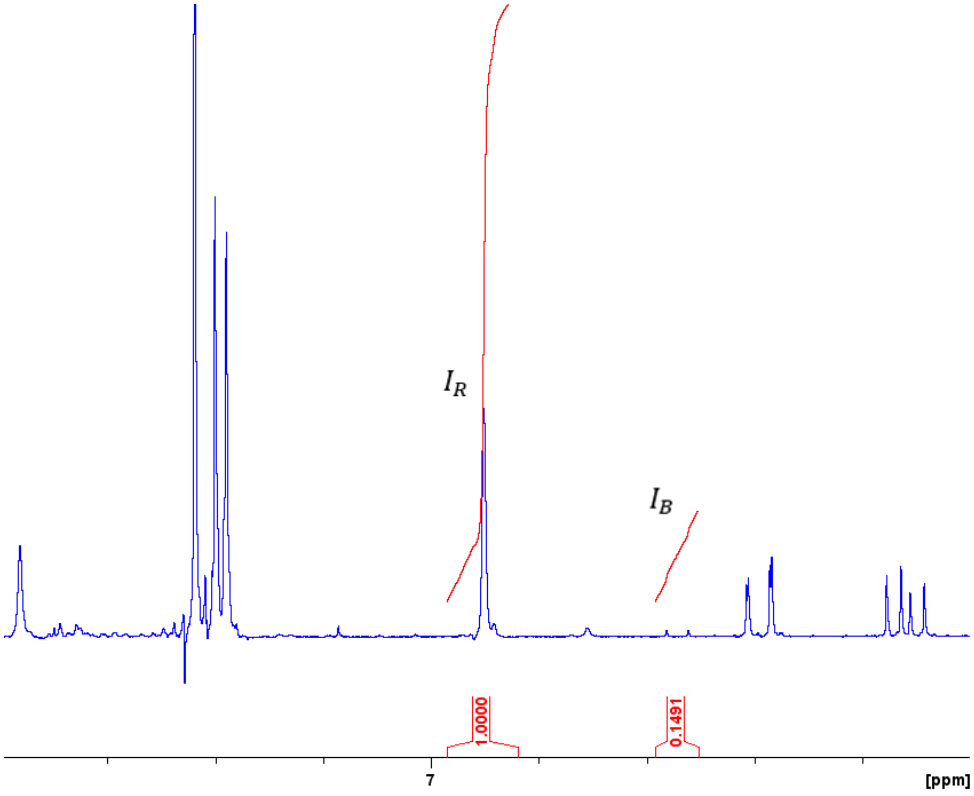

Figure A-26 ^{1}H NMR spectrum of a reaction mixture of 4-iodobenzonitrile and methyl acrylate using 3-Py-BDP-Pd as a catalyst. The spectrum was collected in $CDCl_3$

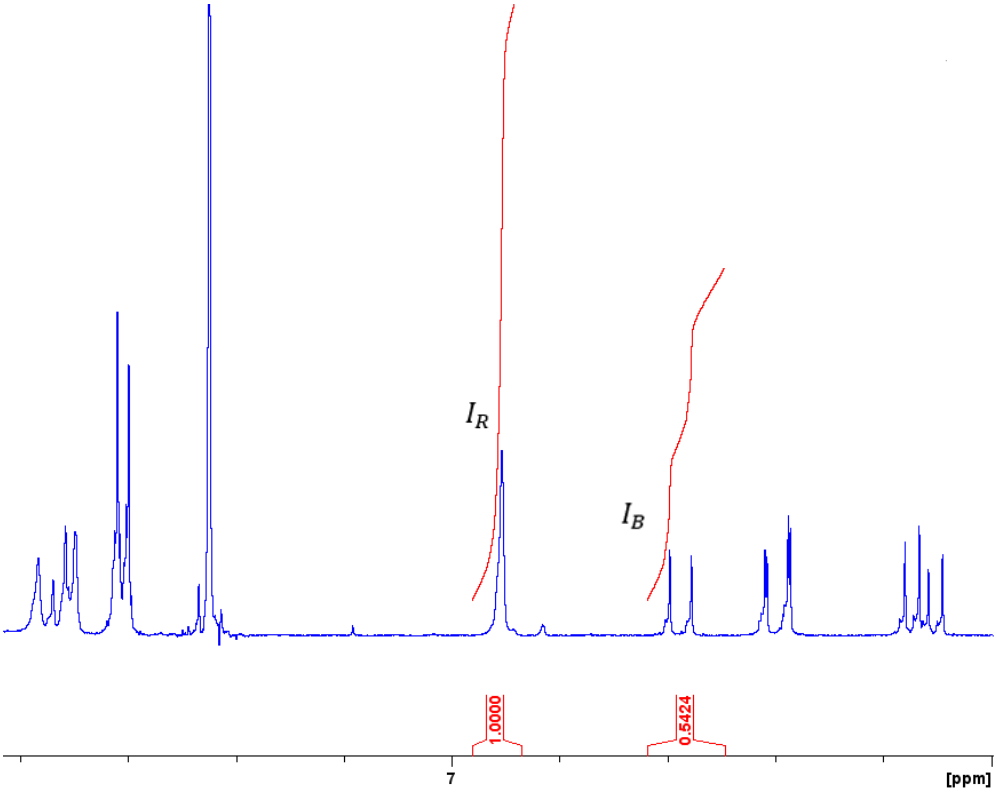

Figure A-27 ^{1}H NMR spectrum of a reaction mixture of 4-iodobenzaldhyde and methyl acrylate using 3-Py-BDP-Pd as a catalyst. The spectrum was collected in $CDCl_3$

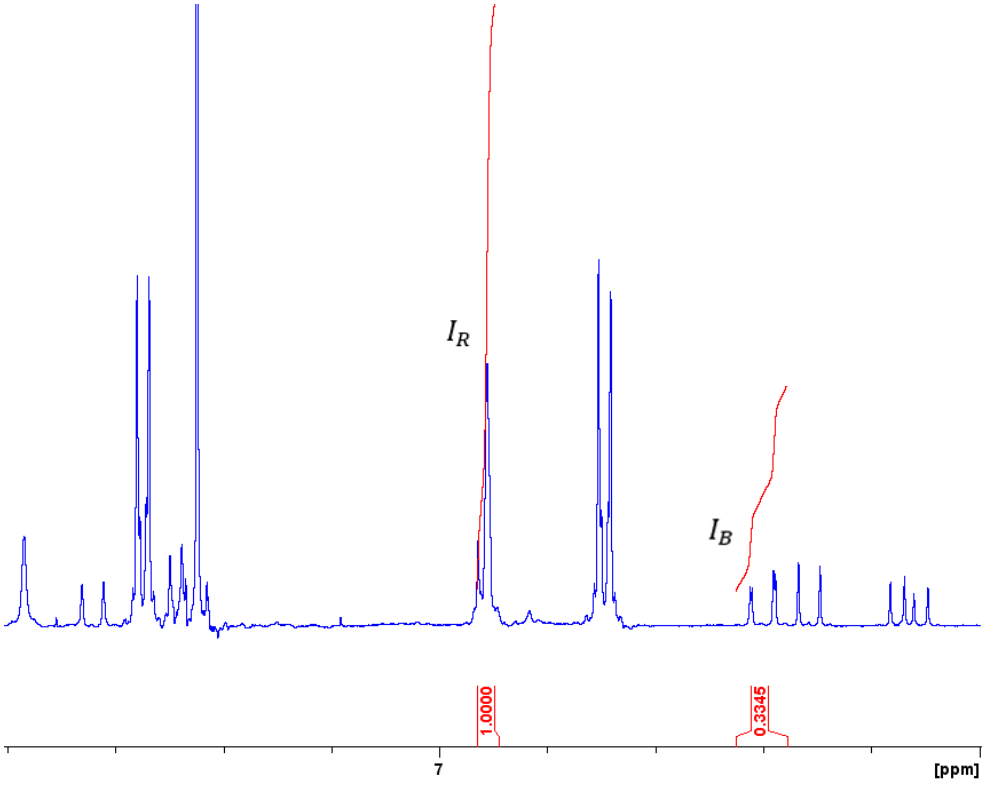

Figure A-28 ^{1}H NMR spectrum of a reaction mixture of 1-iodo-4-methoxybenzen and methyl acrylate using 3-Py-BDP-Pd as a catalyst. The spectrum was collected in $CDCl_3$

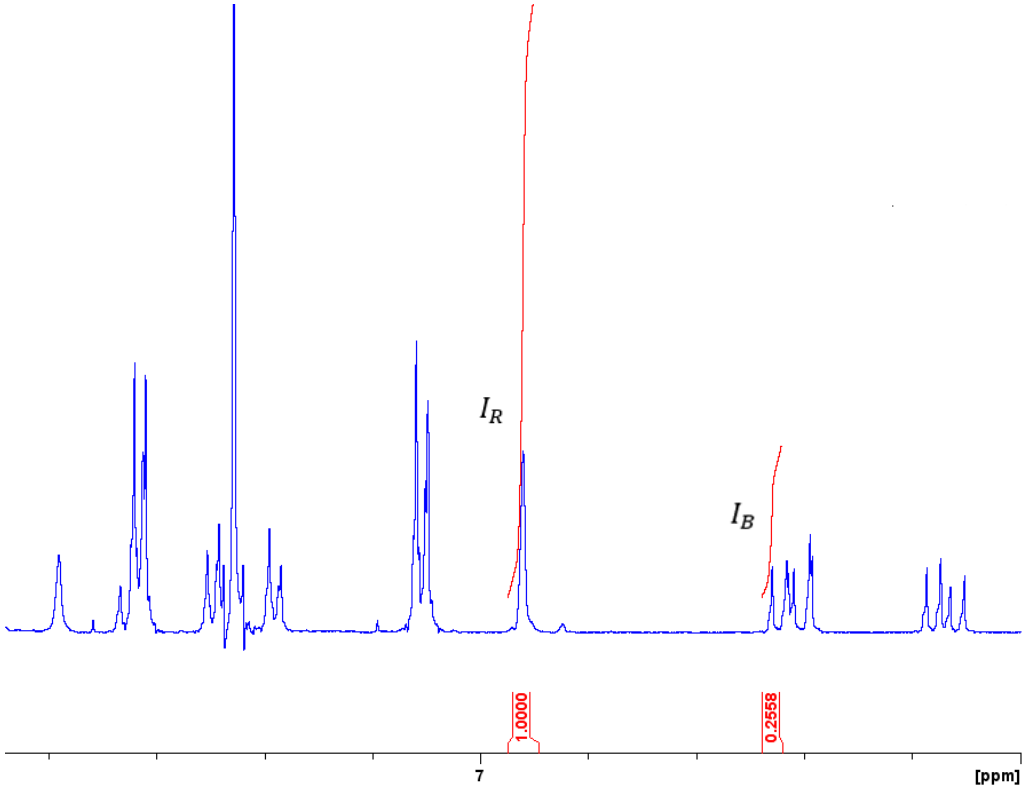

Figure A-29 ^{1}H NMR spectrum of a reaction mixture of 1-chloro-4-iodobenzene and methyl acrylate using 2-Py-BDP-Pd as a catalyst. The spectrum was collected in $CDCl_3$

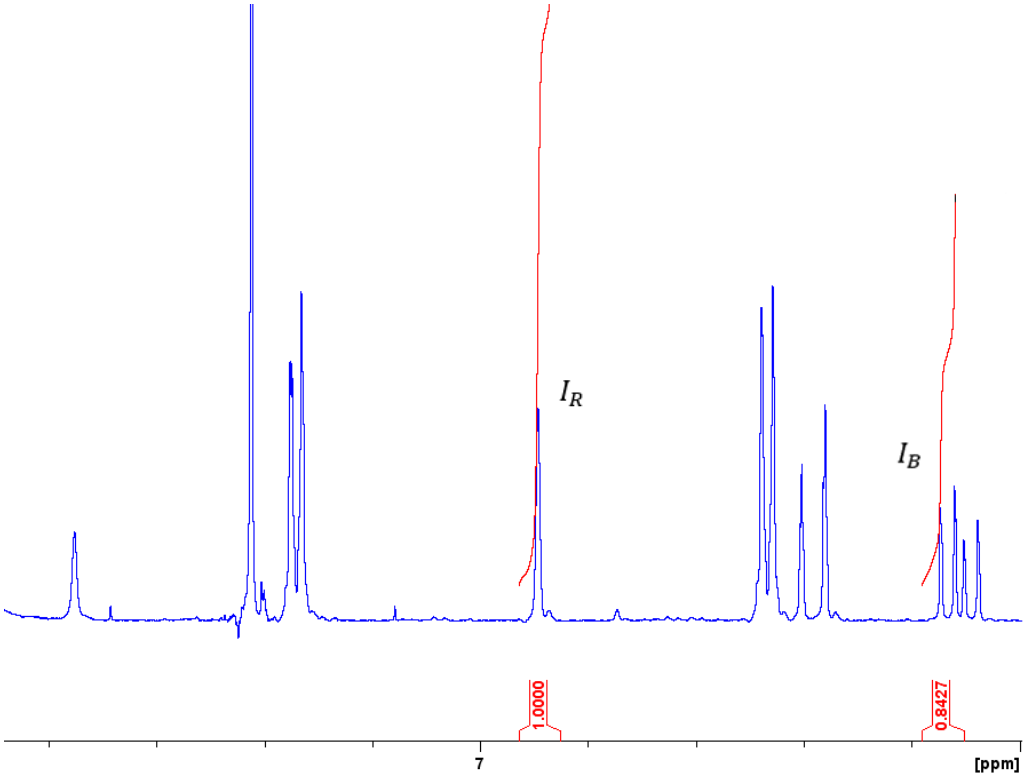

Figure A-30 ^{1}H NMR spectrum of a reaction mixture of 4-iodoaniline and methyl acrylate using 2-Py-BDP-Pd as a catalyst. The spectrum was collected in $CDCl_3$

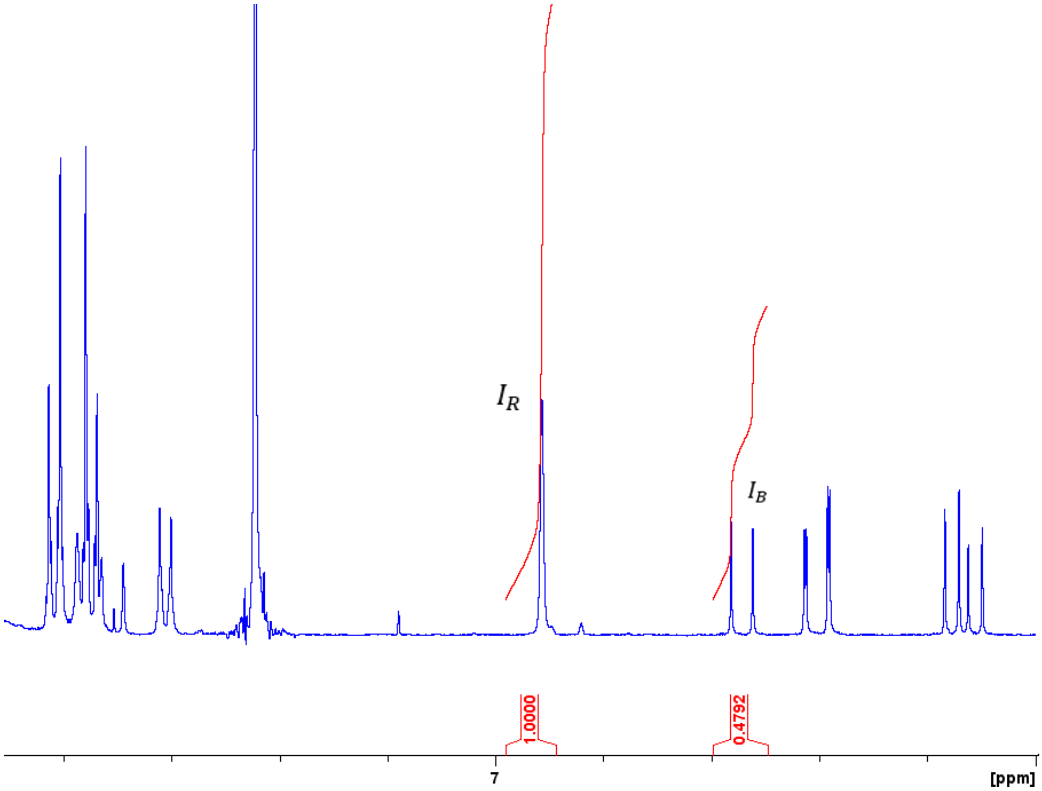

Figure A-31 ^{1}H NMR spectrum of a reaction mixture of methyl-4-iodobenzene and methyl acrylate using 2-Py-BDP-Pd as a catalyst. The spectrum was collected in $CDCl_3$

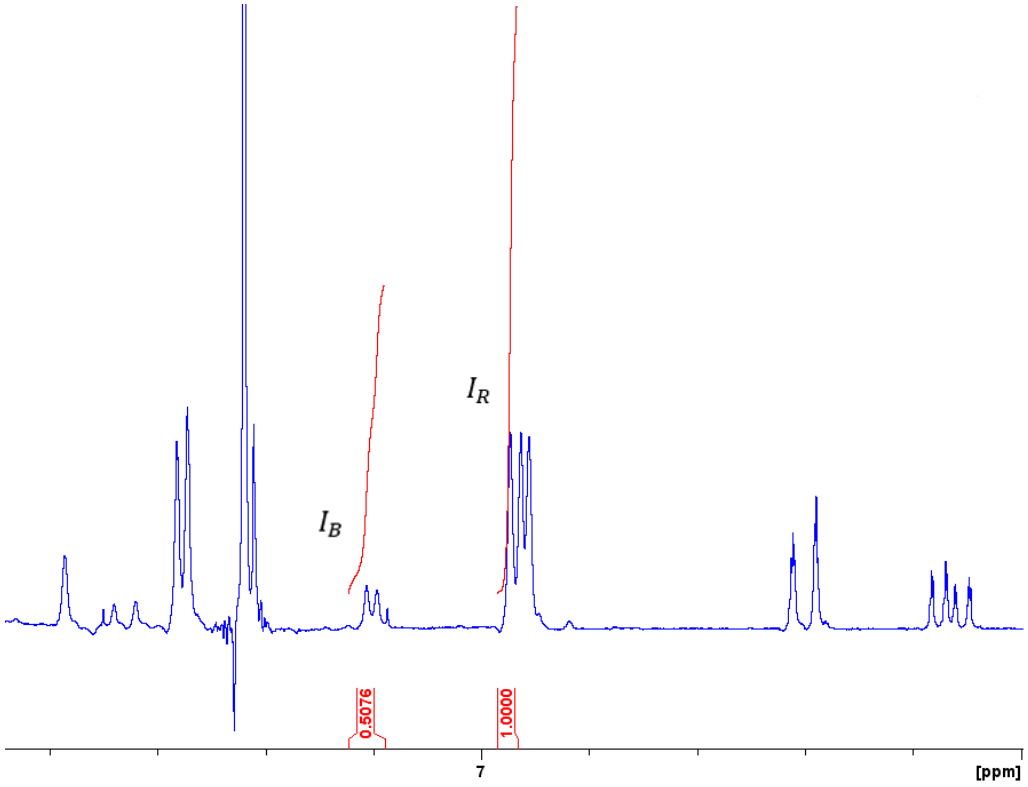

Figure A-32 ^{1}H NMR spectrum of a reaction mixture of 4-iodotoluene and methyl acrylate using 2-Py-BDP-Pd as a catalyst. The spectrum was collected in $CDCl_3$

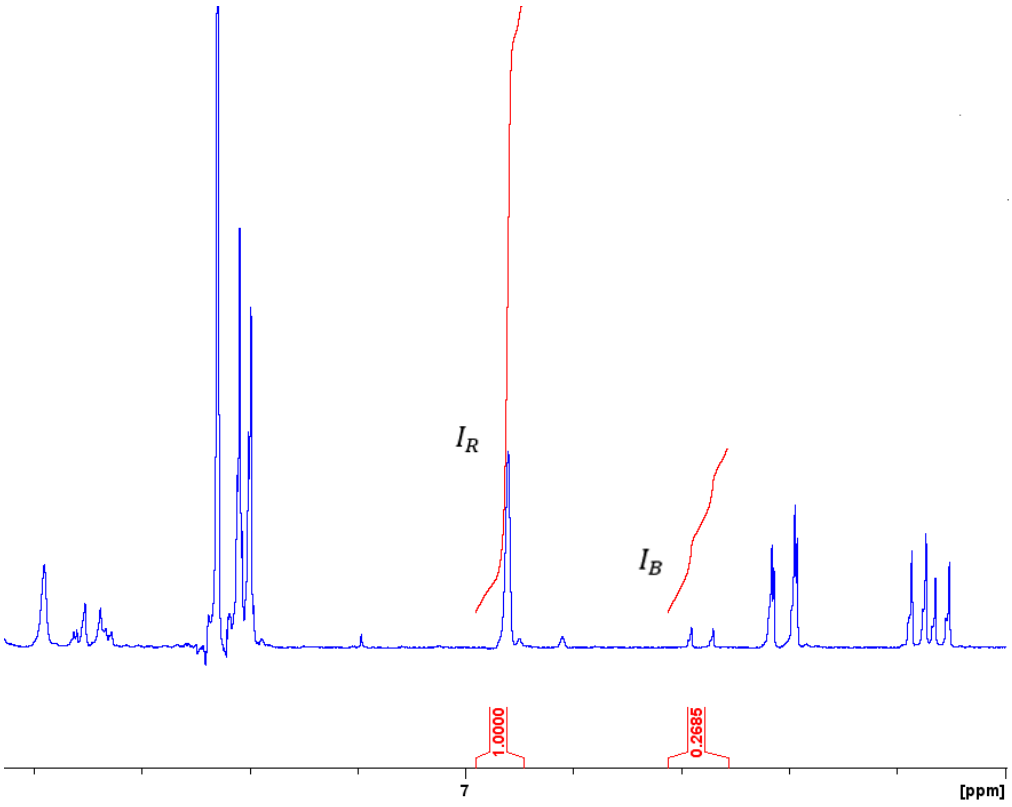

Figure A-33 ^{1}H NMR spectrum of a reaction mixture of iodobenzonitrile and methyl acrylate using 2-Py-BDP-Pd as a catalyst. The spectrum was collected in $CDCl_3$

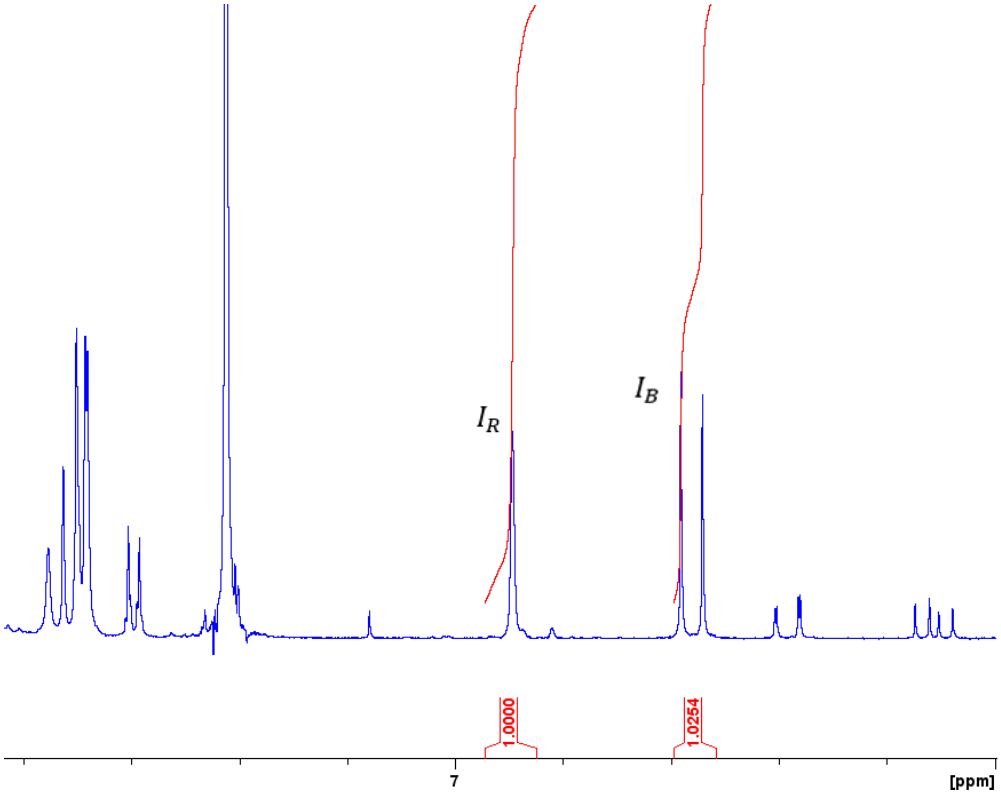

Figure A-34 ^{1}H NMR spectrum of a reaction mixture of 4-iodobenzaldhyde and methyl acrylate using 2-Py-BDP-Pd as a catalyst. The spectrum was collected in $CDCl_3$

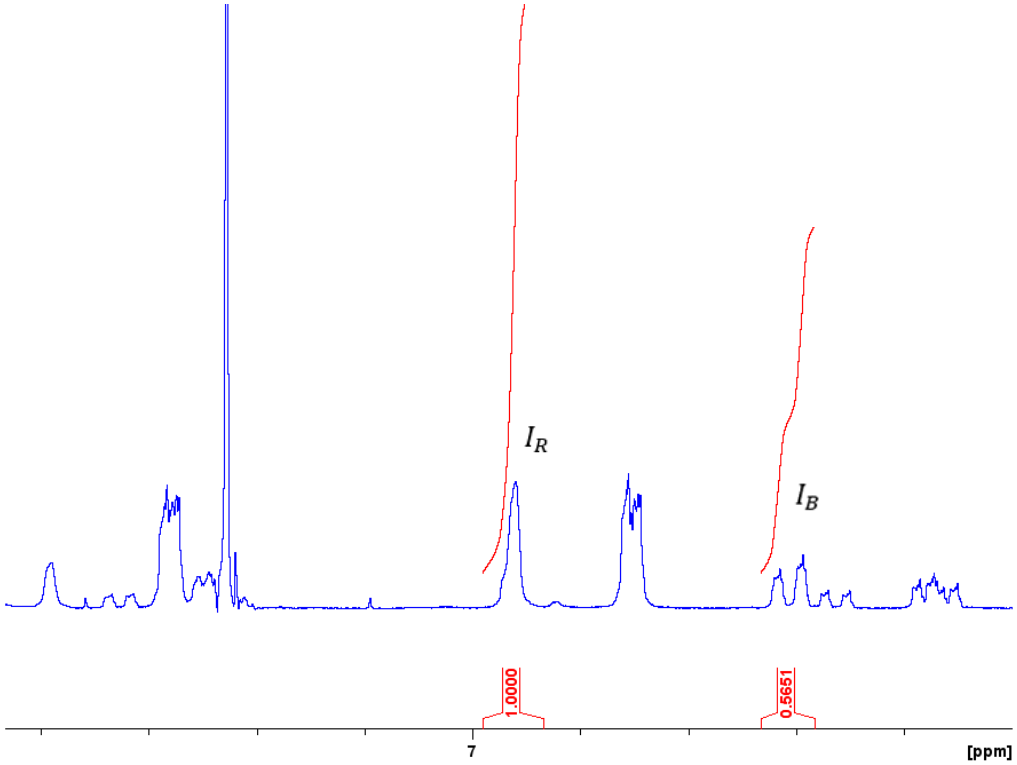

Figure A-35 1H NMR spectrum of a reaction mixture of 1-iodo-4-methoxybenzen and methyl acrylate using 2-Py-BDP-Pd as a catalyst. The spectrum was collected in CDCl3

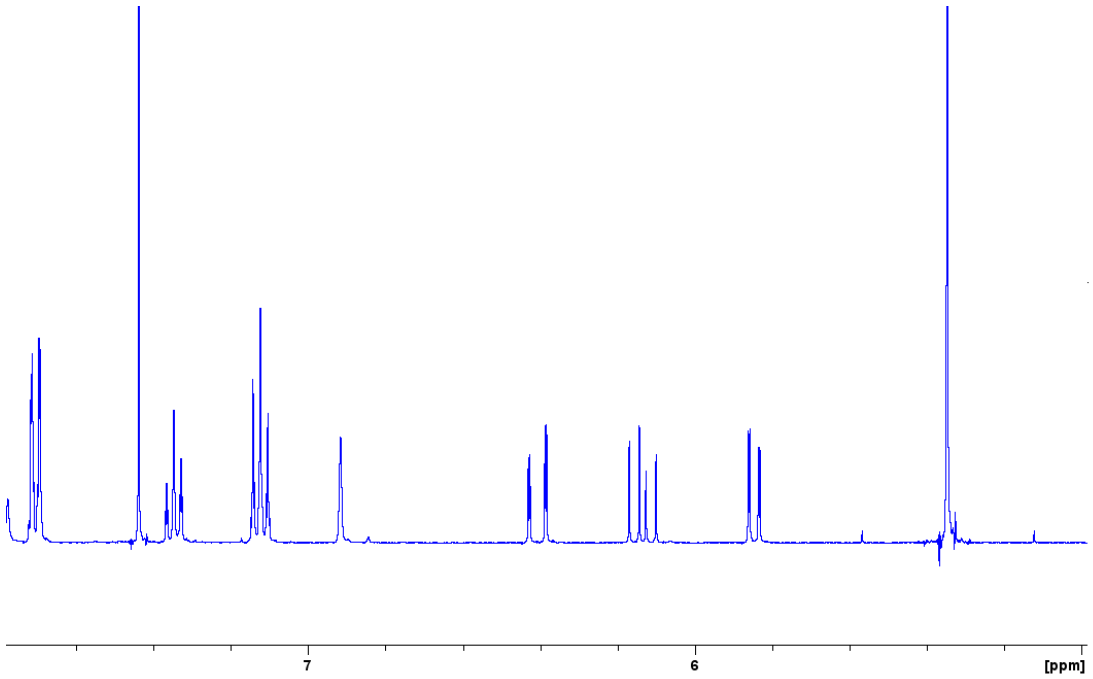

Figure A-36 ^{1}H NMR spectrum of a reaction mixture of iodobenzene and methyl acrylate using 4-Py-BDP-Pd as a catalyst with no base. The spectrum was collected in $CDCl_3$

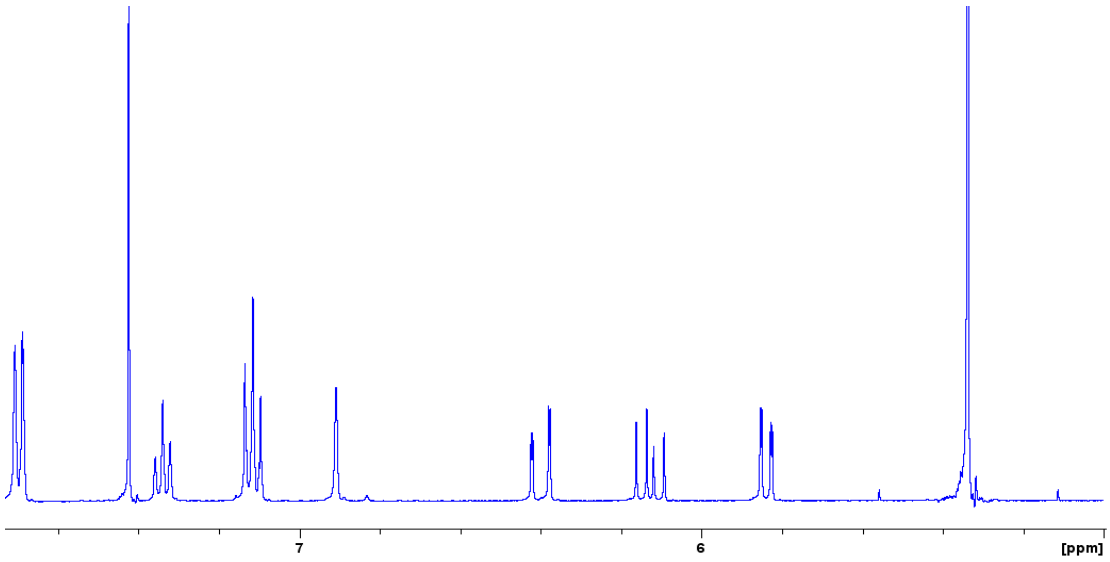

Figure A-37 ^{1}H NMR spectrum of a reaction mixture of iodobenzene and methyl acrylate using 4-Py-BDP-Pd as a catalyst with no base. The spectrum was collected in $CDCl_3$

The method below was used to calculate yield % from ^{1}H NMR analysis. The moles of the product can be determined using the following equation:

$$m_B = m_R\left(\frac{\frac{I_B}{n_B}}{\frac{I_R}{n_R}}\right)$$

$m_B = mol\ of\ product$

$m_R =\ moles\ of\ reference\ being\ added$

$n = corresponding\ No.of\ Hs$

$I_B = integration\ of\ product$

$I_R = integration\ of\ standard\ refernce$

Then yield can be calculated from the equation below

$$Yield\ \% = \frac{(m_B)}{(m_A)} \times 100\%$$

$$m_A = \ moles\ of\ \ corresponding\ starting\ material$$

Reaction conditions: 0.50 mol methyl acrylate, 0.50 mmol iodobenzaldehyde in 2.00 ml of DMF for the reaction. 50 µL of the reaction mixture and 20 µL in reference in 0.5 ml of $CDCl_3$ for ^1H NMR. Reference: 1.00 mmol of trimethyl benzaldehyde in 4.00 ml of DMF.

m_A = (0.50 mmol) (50/2000) =0.0125 mmol

= (1.00 mmol) (20/4000) = 0.005 mmol

To calculate entry 6 from table 3-3

$$m_B = m_R\left(\frac{\frac{I_B}{n_B}}{\frac{I_R}{n_R}}\right) = (0.005mmol)\left(\frac{\frac{0.3588}{1}}{\frac{1.00}{2}}\right)$$

=2.588×10^{-3} mmol

Yield (%) = (100) × (2.588×10^{-3}/0.0125) %= 29%

Table A-1 Calculation for table 3-3

Entry	I_B	I_R	m_R	m_A	m_B	$Yield\ \%$
4	0.1268	1.00	0.005	0.0125	1.268×10^{-3}	10%
5	0.1603	1.00	0.005	0.0125	1.603×10^{-3}	13%
6	0.3588	1.00	0.005	0.0125	2.588×10^{-3}	29%
7	0.5704	1.00	0.005	0.0125	5.704×10^{-3}	46%
8	0.3509	1.00	0.005	0.0125	3.509×10^{-3}	28%

Table A-2 Calculation for table 3-4

Entry	I_B	I_R	m_R	m_A	m_B	$Yield\ \%$
1	0.2261	1.00	0.005	0.0125	2.261×10^{-3}	18%
2	1.0017	1.00	0.005	0.0125	0.0100	80%
3	0.7789	1.00	0.005	0.0125	7.789×10^{-3}	62%
4	0.3521	1.00	0.005	0.0125	3.521×10^{-3}	28%
5	0.1437	1.00	0.005	0.0125	1.437×10^{-3}	11%
6	0.7676	1.00	0.005	0.0125	7.676×10^{-3}	61%
7	0.9217	1.00	0.005	0.0125	9.217×10^{-3}	74%
8	0.4634	1.00	0.005	0.0125	4.634×10^{-3}	37%
9	0.1218	1.00	0.005	0.0125	1.218×10^{-3}	10%
10	0.3785	1.00	0.005	0.0125	3.785×10^{-3}	30%
11	0.6902	1.00	0.005	0.0125	6.902×10^{-3}	55%

Table A-3 Calculation for table 3-5

Entry	I_B	I_R	m_R	m_A	m_B	$Yield\ \%$
1	0.2913	1.00	0.005	0.0125	2.913×10^{-3}	23%
2	0.6718	1.00	0.005	0.0125	6.718×10^{-3}	54%
3	0.6633	1.00	0.005	0.0125	6.633×10^{-3}	53%
4	0.1491	1.00	0.005	0.0125	1.491×10^{-3}	12%
5	0.5424	1.00	0.005	0.0125	5.424×10^{-3}	43%
6	0.3345	1.00	0.005	0.0125	3.345×10^{-3}	27%

Table A-4 Calculation for table 3-6

Entry	I_B	I_R	m_R	m_A	m_B	$Yield\ \%$
1	0.2558	1.00	0.005	0.0125	2.558×10^{-3}	20%
2	0.8427	1.00	0.005	0.0125	8.427×10^{-3}	67%
3	0.4792	1.00	0.005	0.0125	4.792×10^{-3}	38%
4	0.5076	1.00	0.005	0.0125	5.076×10^{-3}	41%
5	0.2685	1.00	0.005	0.0125	2.685×10^{-3}	21%
6	1.0254	1.00	0.005	0.0125	0.0102	82%
7	0.5651	1.00	0.005	0.0125	5.651×10^{-3}	45%